MASTER THESIS

DYNAMIC ANALYSIS OF CONCRETE ARCH BRIDGES UNDER HIGH SPEED TRAIN LOADS

Case study: viaduct over the Almonte river

By:
María Macías Infantes
Civil Engenieer

Advisor:
Dr. Alejandro E. Martínez Castro

Department of Structural Mechanics and Hydraulic Engineering
ETS de Caminos, Canales y Puertos
University of Granada

Granada, September 2017

This work has been done as a part of the Master's Degree in Structures at the University of Granada. The work has been supervised by Prof. Dr. Alejandro E. Martínez Castro, who has developed the main tool used in this research. On this work I have included the results of my own work.

The work presented here includes a review of the state of the art of the methods to obtain the dynamic response of a bridge under high speed train loads. A semi-analytic method proposed by the tutor of this thesis has been used through a complete case study of a concrete arch bridge.

María Macías Infantes

Abstract

This work analyses the dynamic response of high-speed railway (HSR) bridges through a case study: the viaduct over the Almonte River on the HSR line from Madrid to Lisbon. The main objective is to develop a methodology for the dynamic analysis of HSR arch bridges based on the semi-analytic method proposed by Martinez-Castro et al. and analyze their specific behavior.

Firstly, it is refered the way the dynamic study of HSR bridges is treated in instructions. Also the semi-analytic method is described.

Secondly, five different finite element models of the Almonte bridge are developed, including one considering the soil-structure interaction.

Finally, the dynamic response of the bridge is analysed through the different models and conclusions are drawn on the suitability of the different models.

Keywords: *high-speed railway bridges, dynamic analysis, semi-analytic method, dynamic impedances, Finite Element models.*

Resumen

El presente trabajo se encarga de analizar la respuesta dinámica de puentes de ferrocarril para alta velocidad (AV) a través del estudio de un caso práctico: el viaducto sobre el río Almonte de la línea de AV Madrid-Lisboa. El objetivo principal es desarrollar una metodología para el análisis dinámico de puentes arco de ferrocarril para AV basada en el método semi-analítico propuesto por Martínez-Castro et al. y analizar su comportamiento específico.

En primer lugar se resume cómo se aborda en la normativa el estudio dinámico de puentes de ferrocarril y se describe el método semi-analítico.

En segundo lugar se realizan cinco modelos diferentes de elementos finitos del puente sobre el río Amonte, incluido uno considerando la interacción suelo-estructura.

Por último se analiza la respuesta dinámica del puente a través de los diferentes modelos y se sacan conclusiones sobre la idoneidad de los diferentes modelos.

Palabras clave: *Puentes de ferrocarril para alta velocidad, análisis dinámico, método semi-analítico, impedancias dinámicas, modelos de Elementos Finitos.*

Acknowledgements

I would like to express my gratitude to Prof. Dr. Alejandro E. Martínez Castro for his guidance and for all the knowledge provided during this months.

Dedicated to my family and my partner for all the support and encouragement they always give me.

Muchas gracias.

Contents

List of Figures

List of Tables

CHAPTER

1

Introduction

1.1 Introduction

Motivation

Since the origin of railways in Europe during the Industrial Revolution at the beginning of the 19th century, the speed of passenger trains became an essential argument for companies and countries to compete. After some significant speed records in Europe, in October 1964 Japanese national railways started the operation of the Tokaido Shinkansen line, from Tokio Central to Shin Osaka. This line was designed to operate at 210 km/h and it also had modern control systems. This can be considered the birth of the High Speed Rail (onwards HSR).

Shortly after the success of the Shinkansen line, innovations and new technologies developed in several European countries established the basis for the "passenger railway of the future". It was in 1981 when the national French railway company started the operation of the first high speed line between Paris and Lyons: the TGV. During the journey, the train reached a maximum speed of 260

km/h. It was the birth of the European HSR. The main difference between the Shinkansen and the European HSR lines was that the first one was a fully brand new line while the second was fully compatible with existing railways. Thats's why the HSR suffered a great further development in most European countries and each one looked for the new generation of competitive long and medium distance passenger rail services.

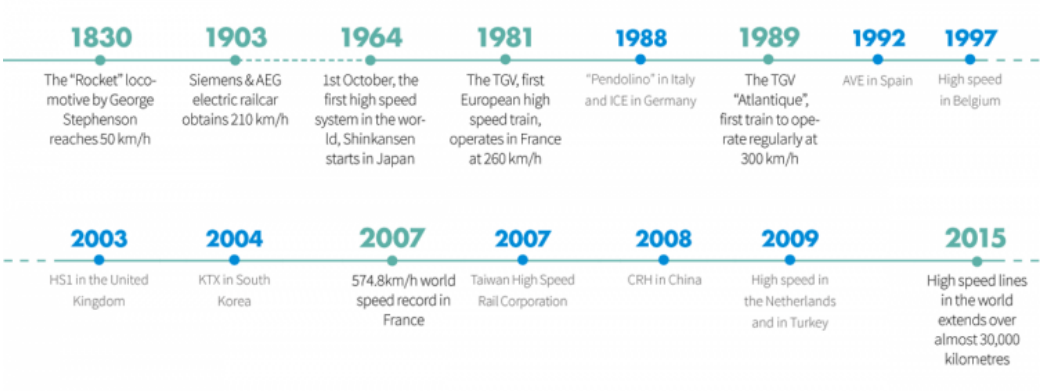

Figure 1.1: Main events in the HSR history. Source: `http://uic.org/High-Speed-History`.

Here in Spain the HSR was introduced in the late '80s, taking inspiration from French model. The first project so-called N.A.F.A. (the acronym in Spanish of *Nuevo Acceso Ferroviario a Andalucía*) was opened up in april 1992, matching with the Universal Exposition of Seville (Expo '92). This HSR line named AVE (*Alta Velocidad Española*) allowed to get in Seville from Madrid in just three hours. From then on, the number of HSR lines in Spain has been increased a lot and nowadays it exists a very functional radial network as it can be seen in the figure 1.2.

The High Speed Rail changes the concept of long travel, greatly reducing travel times. Therefore, HSR lines represent one of the most important infrastructures in development plans. In fact, in the last transportation planning called *Plan de Infraestructuras, Transporte y Vivienda 2012-2024*, railway transport count on more than 60.000 million euros, that represents 44% of the plan's budget.

Figure 1.2: Map of the Spanish high-speed railway network. Source: `https://es.wikipedia.org/wiki/Archivo:HighSpeedSpain.svg`.

On the other hand, to achieve a useful railway transport and make it more comfortable for passenger and functional in freight transport the regulation called IAPF-07 was pass in 2007. This document establishes some dynamic limitations in vertical accelerations, maximum deflection and warping in ballasted decks of high speed railway bridges. To checkup this restrictions, it is necessary to solve the dynamic problem considering a moving load. The traditional way to solve this kind of problems is by using a numerical integration method, usually Newmark-Beta method. The problem is that numerical integration algorithms have an incremental formulation so its precision depends on the temporal discretization. Nevertheless there is a revolutionary semi-analytic method to solve the moving load problem proposed by the advisor of this Master Thesis that allows to carry out all the load cases imposed in the instruction by not discretizing the time domain.

For all this reasons, the main motivation of this document is to perform a

practical dynamic computation using the semi-analytic method and show its advantages. Besides, the case study chosen consist in a concrete arch bridge of a high speed line built in Spain. This type of bridge is interesting from an engineering point of view because there are not many of them in the high speed railways in Europe. Furthermore, spatial arch bridges have significant out-of-plane behavior so its dynamic response can be decisive for its own design.

Special features of railway arch bridges

Ideally, an arch is an structure that is only subject to compressive stress, free of any bending moments and shear stress. If so, the arch is absolutely efficient because every part of its cross sections is subject to the same stress and there are no wasted parts. In order to obtain an ideal arch free of bending moments, the arch shape must coincide with the line of thrust caused by loads acting on it. But in real arch bridges there is no single line of thrust because all the different load cases. And what's more, moving loads causes changes in the line of thrust. Hence differences between the arch axis and the line of thrust are unavoidable and there are always bending moments that could be important in some cases. Thus it is important to ensure enough bending resistance but also checking bucking problems derived from the compressive stress.

Usually arch bridges are classified into three types namely:

- Deck arch bridges: the arch is located below the deck.
- Through or tied arch bridges: the arch is situated above the deck.
- Half-through arch bridges: there are parts of the arch below and above the deck.

Another important issue of arch bridges is how to carry loads to the ground. Deck bridges usually require a very competent foundation to support the high vertical and horizontal forces transmitted by the arch. This issue is less important

in through and half-through arch bridges because the deck tie the horizontal thrust of the arch.

Arch bridges for HSR are deck arch bridges and they usually are pointed arches. The use of this type of arch started to be used in the Middle Ages with the gothic style. A concentrated load on top of the key is needed to maintain its structural efficiency. The HSR bridges have much more requirements than highway bridges. First of all, train loads are higher than traffic loads and they are many types of trains with different arrangement of load axles. This makes it more difficult to obtain an accurate inverse funicular curve for the arch thus higher bending moment could appear. Secondly, the dynamic effect caused by the high speed trains could also be limiting. Finally, the limitations for service deflections and acceleration stablished in the instruction are very strict.

Recently, three outstanding deck bridges have been built in Spain: Contreras Reservoir Bridge, Alcántara and Almonte River Bridge. The three are deck arches erected by the cable-stayed cantilever method, and the last one represents the case study of this document.

1.2 Objectives and main contributions

The main objectives of this Master Thesis may be summarized at the following items:

- Development of a methodology for the dynamic analysis of HSR arch bridges based on the semi-analytic method proposed by Alejandro Martínez Castro et al., which includes all verifications established in the current regulation (IAPF-07).
- Analysis of the specific behavior of HSR arch bridges taking into account dynamics effects: arch-deck low-frequency modes, torsion modes derived from the off-centered moving load over the deck, continuos and maximum deflections and accelerations induced by high speed trains,...

- Elaboration of different finite element models (onwards FE models), including isolated arch models by using 1D and 2D elements and complete models, to get the suitable one for this kind of problems.

- Incorporation of soil-structure interaction models (onward SSI models) to ponder the way its effects attenuate the dynamic response of the arch bridge.

1.3 Organization of this document

This document is organized by independent chapters, in order to present separately the review of the state of the art, the formulation used, the case study and the conclusions. References to general methods, such as Finite Element Method or Boundary Element Method have been omitted. The reader can look for the selected lectures on each chapter to find information about this topics.

The first chapter after this introduction is focused on the available methods to perform dynamic analysis of railway bridges. Some simplified methods proposed in the instruction are presented and also other traditional *step by step* methods.

The Chapter 3 is about the semi-analytic method proposed by the advisor of this Master Thesis. The formulation and solution method is exposed. Also numerical test are shown to confirm the adequate implementation of the theoretical development.

At Chapters 4 and 5 the dynamic analysis of the HSR bridge over the Almonte river is develop. For this propose all tools presented in previous chapters are used and results are analyze.

Finally Chapter 6 presents the main conclusion of this work and also points out some future works related with this research.

CHAPTER

2

Dynamic analysis of railway bridges

2.1 Introduction

Generally all brand new structures and specifically railway bridges tend to be more and more slenderness. Thus dynamic effects become very important, even more in HSR bridges because the high speed moving loads. Therefore, national regulations are concerned about dynamic problems.

This dynamic effects can affect the passengers comfort, but also could endanger the ballasted track. In some cases, dynamic effects could condition the structural design.

2.2 The dynamic problem in Spanish regulation

Current Spanish legislation called IAPF-07 poses several methods to evaluate dynamic effects. Articles and formulas indicated in this section can be found in the text of the instruction [2] .

Dynamic effects are not taken into account directly. For this propose, so-called impact coefficient Φ is defined and it is used to increase static loads. The general formula for this coefficient is expressed by equation 2.1.

$$\Phi = \frac{\max(S_{din,real})}{S_{est,tipo}} \tag{2.1}$$

where:

$\max(S_{din,real})$: Maximum dynamic load derived from all kind of real trains running at any speed.

$S_{est,tipo}$: Static load owing to UIC71 train defined in 2.3.1.1 placed in the most adverse position.

To calculate Φ coefficient, the following two cases may be considered. This methods are detailed in next section.

1. Trains running at speed $v <= 220$ km/h
   - For conventional bridges satisfying the frequency limitation defined in B.4, it can be used a simplified method known as *enveloped of impact coefficients method*.
   - In another case, it is necessary to employ the *impact coefficient method for the actual trains*.
2. Trains running at speed $v > 220$ km/h:
   - For isostatic bridges the *dynamic signature method* can be used.
   - In another case it is necessary to carry out a dynamic analysis, using the general time domain integration method for moving loads.

2.2.1 Enveloped of impact coefficients method

This is the most simplified method. The impact coefficient can be compute by using expressions B.5 or B.6 in the instruction. This coefficient represents an enveloped of coefficients obtain for many problems of different actual bridges. Therefore, the use of this method is limited to conventional structures. In this cases it is also assume there isn't resonant phenomenas and accelerations don't overcome the allowable limit.

2.2.2 Actual trains impact coefficient method

Whereas the above method provide a single impact coefficient for all trains and speeds, this method provides an impact coefficient for each actual train, which is more accurate. There are two options to obtain this coefficients:

a) By using analytical expession B.13.

b) Carrying out a general dynamic analysis for trains defined in annexed C.3 of the instruction. Any of the following methods could be used to develop the dynamic analysis.

2.2.3 Dynamic signature method

This is also a simplified method, so it only can be used for isostatic bridges and other special structures. Maximum dynamic response can be obtain as the product of two functions with analytical expressions. There are two different methods: DER and LIR. Information of this methods can be found in documents working out by ERRI (European Rail Research Institute) and also in [3].

2.2.4 General time domain integration method

This method characterizes trains as moving loads to define a general time domain dynamic problem. Hence, is the most general approach and it is valid for all singular problems.

The aim is to determine the most unfavorable loading situation (enveloped), simulating the traffic at different speeds, from 20 km/h to 1.2 times the design speed. The increase of speed between each step will be less than 10 km/h. Th HSLM (High Speed Load Model) defined in the Eurocode 1 [4] is used for this propose.

Finally the impact coefficient can be compute using the following equation:

$$\Phi = \frac{\delta_{din,real}^{ideal}}{S_{est,tipo}} \cdot (1 + r\phi'')$$

where:

r: coefficient which depends on the track maintenance, defined by expression B.11 in the instruction.

ϕ'': coefficient which represents the track irregularities, defined by expression B.12 in the instruction.

This method can be completed including vehicle-structure interaction. In this kind of models, the load is considerate variable to take into account the train suspension system. It can be useful in some special situations or as a part of a research work, but in practice this models are too much complex. The coefficients obtain with this models are usually lower in isostatic bridges, but the interaction has no much effect in hyperstatic structures.

2.3 Approaches to moving load problems

2.3.1 Research and recent papers

The dynamic behaviour of structures under moving loads is a problem of interest in the field of railway and highway bridges design. In this problems, traffic load are represented as constant concentrated loads moving on a line at constant speed.

The first time this models were proposed was at the beginning of the 20th century, when first steps towards HSR were come about in Europe [5, 6]. It is a complex problem whereby exact solution only exists for some simple cases such as isostatic structures [7, 8, 9].

It is more difficult to find some papers about exact solutions for hyperstatic structures. Some examples are the research by Hayashikawa and Watanbe for multispan nonuniform beams and the work by Chen and Li for specific exponential loads [10]. Another remarkable work is the one realized by Henchi [11], who obtained the frequency domain solution.

Over time the dynamic problem have been faced with approximate methods. For general loads over a general structure, step-by-step methods are the popular ones (see [12] for more informations about this topic). Particularly the integration method so-called Newmark-Beta is the most used one in dynamics of structures [13].

Since the definition of Newmark-Beta technique in 1959, it has been employed in many applications. Among the large number of papers using this method, the work made by Liu et al. [14] about Sesia viaduct must be taken into account. It is a very complete research in which vehicle-structure interaction is considered in the numerical model and it also includes in situ test results after construction. Paper conclusions about damping of this type of structures are very interestig.

The main problem of direct integration technique is because of the time dis-

cretization. Time step have to be very small to obtain accurate solutions, so the computational cost is too much large in many cases. To overcome this problem, some other methods have been proposed.

Dugush and Eisenbeg [15] presented in 2002 a new approach to the problem. The propose consists on describing vibration modes by infinite polwer series. Thereby the spatial problem is solved exactly by using dynamic direct stiffness method and the temporal solution is analytical.

Another semi-analytic alternative method was proposed in 2003 by Martinez-Castro et al. [16, 17, 18]. In this methodology structure is spatially discretized using the conventional finite elements. Then, the (approximate) mode shapes and natural frequencies are computed using standard eigensolution procedure. Finally, the equivalent modal loads are expressed analytically in terms of the previously computed mode shapes. This leads to the mathematical expression of the time domain solution for each mode in a straightforward manner. For this reason, errors due to temporal discretization are avoid. The semi-analytic method have been encourage by the scientific community and it has been successfully used in the design of the Santa Ana bridge [19]. Chapter 3 of this document is focused on the formulation of the semi-analytic method.

2.3.2 **Theoretical background: time domain integration methods**

A general dynamic problem solution of a moving load is obtained using numerical integration. There are two different methodologies:

- Direct methods:

  This are the most general methods because they allow non-linear behaviour. This techniques consists in the direct integration of the equilibrium equations for all degrees of freedom (DOF) of the structure at every time.

Some popular direct methods are step-by-step algorithms such as Newmark-Beta, Hughes or Wilson method. Some references about this topic are [13, 20, 21, 22].

- Indirect methods:

  On the other hand, indirect methods use the superposition principle so they are only useful for linear behaviour. This technique consists in the use of modal analysis to decouple the DOF and to separate the spatial and temporal variables. Except for very simple load cases, it will not possible to solve the temporal problem analytically, so the use of a step-by-step method is unavoidable.

2.3.3 Step-by-step integration methods

Step-by-step methods have different formulations but all are based on the division of the load and the system response in a set of sequential time steps. The response at the current step is compute from the response in the previous steps in a certain way.

The initial equation for a first order temporal integration algorithm, also known as Cauchy problem is:

$$\dot{y}(t) = f(t, y(t)), y(y_0) = y_0; t \in [t_0, t_f]$$

However to solve a dynamic problem it is necessary to use second order temporal integration algorithms. In this case, the initial equation is:

$$M \cdot \ddot{w} = F(w, \dot{w}, t)$$

where array F and matrix M are generally non-linear functions of $(w, \dot{w}, t)$. To transform this second order problem in a first order one it is used the next conversion:

$$y = \frac{w}{\dot{w}} \longrightarrow \dot{y} = \frac{\dot{w}}{M^{-1} \cdot F(w, \dot{w}, t)} = F(t, y(t))$$

Temporal integration methods estimate the current solution from information at previous steps. In this way, solution $y_n\,(n = 0, 1, ..., N)$ at time step t_n is obtained from solution in preceding k steps.

$$\sum_{j=0}^{k} \alpha_j y_{n+j} = h \cdot \Phi(y_{n+k}, y_{n+k-1}, y_{n+k-2}, ..., y_n, t_{n+k}; h_{n+k}) \tag{2.2}$$

Equation 2.2 is the most general form of a step-by-step method. This methods can be classified according to different criteria:

- One step and multistep methods:

  One step methods are those which obtain the response at step t_n from the information in the step $t_{n-1} = t_n - \Delta t_{n-1}$. The most popular one is the classical Runge-Kutta method.

  Instead multistep methods are those which obtain the response at step t_n from the information in several previous steps. The most used are Adams methods.

- Explicit and implicit methods:

  Explicit methods pose the differential equation at step t_{n+1} to estimate the solution at step t_n. Consequently solution y_{n+k} can be expressed separately from previous solutions $y_{n-j}\,(j = 0, 1, ...k - 1)$. All explicit methods are conditionally stable in terms of time step. That means it is necessary to fix a small enough time step to obtain an stable solution. An example of this numerical integration technique are explicit Runge-Kutta method.

  On the other hand, implicit methods solve the differential equation at step t_n only after the solution in step t_{n-1} has been found. In this case, solution y_{n+k} can't be expressed separately from previous solutions $y_{n-j}\,(j = 0, 1, ...k-1)$ and a linear equation system must be solve at every step. However this methods can be conditionally or unconditionally stable, so higher time sept can be used. Some examples are one step implicit Adams method (known as trapezoidal rule) and Newmark-Beta algorithm.

- Fixed-step and variable-step methods:

  In fixed-step methods the value of time step Δt_n is constant throughout all the performance. All methods designate before are fixed-step methods.

  Otherwise in variable-step methods time step Δ_n can be different at each step. The embedded Runge-Kutta methods or Runge-Kutta-Fehlberg method implement this technique.

2.3.3.1 **Disadvantages**

Step-by-step methodology is based on incremental numerical integration in time domain so this domain is thus approximated. In actual structures this methods are not applicable because it is necessary very small time steps to obtain an accurate solution. In this conditions, numerical performances have an excessive computational cost so only not very large numerical models or detail models can be analyzed by using this technique.

CHAPTER

3

Semi-analytic solution for moving load

3.1 Introduction

The dynamic behaviour of beams under moving loads is of great importance in several fields of engineering, for instance, the design of railway bridges. This topic has become a particular focus area of research because of the appearance of ballast destabilization problems in some European HSR lines. The committee D-214 of the ERRI looked after to analyse these problems and pointed out that the occurrence of intense resonance phenomena associated with flexural oscillations needs further investigation.

With the goal of developing this issue, semi-analytic method was proposed by A. Martínez Castro, P.Museros and A. Castillo-Linares (University of Granada). It was published in Journal of Sound and Vibration in 2006 [1]. In this paper, authors present an alternative method to step-by-step techniques to carry out the analysis of the response of Bernoulli-Euler beams subjected to flexural vibrations

under the presence of concentrated moving forces. Applying this methodology the structure is discretized and the mode shapes are computed using standard procedure. The moving load is represented by a unitary Dirac Delta function, and the modal loads are obtained in terms of cubic Hermitian polynomials. This leads in a straightforward manner to the closed-form solution for the unit load in the time domain. The solution is expressed in terms of 10 coefficients per element and per mode, the values of which are independent of the speed of the moving load. Finally, the response to a series of loads is built simply by adding the contribution of each. The overall procedure is fast and accurate, depending only on the spatial discretization and the time step selected for evaluating the solution without the need of any integration step.

Next paragraphs are focus on the formulation of the semi-analytic solution for beams, but also it is presented a generalized methodology. To finish the chapter, some numerical test have been included in order to show the efficiency of this technique.

3.2 Formulation and semi-analytic solution for beams

In order to expose this new approach to dynamic problems with moving loads, the methodology follow the next items:

1°) Approach to governing equation for non-uniform beams.

2°) Weak and Matrix formulation for a single element.

3°) Assembled formulation.

4°) Solution of the matrix equation system.

5°) Uncoupling the system and solving the equations of motion.

6°) Solution for a set of moving loads.

3.2.1 Governing equation

Let $x \in [0, L]$ be the domain of a Bernoulli-Euler non-uniform beam with a single concentrated load traversing the beam at the constant speed v. This moving load is idealized by means of Dirac Delta function $\delta(x)$. Thus, $p(x,t) = p_0\delta(x - vt)$ represents the effect of a concentrated moving load p_0.

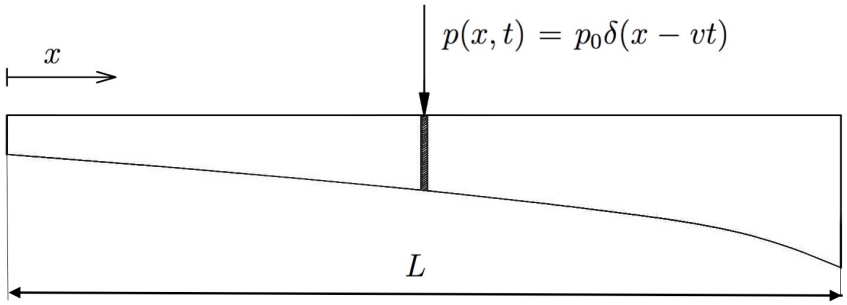

Figure 3.1: Non-uniform beam traversed by a moving load.

At this point, two time intervals are considered: $[0, L/v]$ or forced vibrations, when the load is acting upon the beam, and $[L/v, \infty)$ or free vibrations. During the forced vibration period, the governing differential equation for this beam neglecting damping effects is given by:

$$m(x) \cdot \frac{\partial^2 w(x,t)}{\partial t^2} + \frac{\partial^2}{\partial x^2}[EI(x) \cdot \frac{\partial^2 w(x,t)}{\partial x^2}] + p_0 \cdot \delta(x - vt) = 0 \qquad (3.1)$$

where $m(x)$ stands for the mass per unit length, E is the modulus of elasticity, and $I(x)$ is the variable second moment of area of the cross-section.

Figure 3.2 shows the positive sign of the distributed load, shear force, and bending moment. The displacement function $w(x,t)$ is positive in the upward direction.

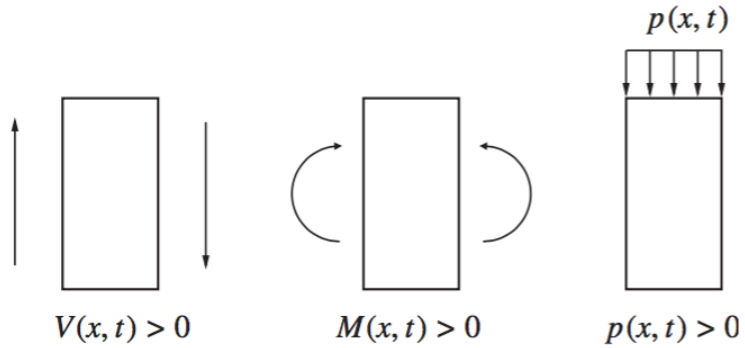

Figure 3.2: Sign convention for the shear force $V(x,t)$, bending moment $M(x,t)$ and load $p(x,t)$. Source: [1].

The boundary conditions for this problem are:

$$w(x,t)|_{t=0} = 0 \quad \forall x \in [0,L] \quad ; \quad \frac{\partial w(x,t)}{\partial t}|_{t=0} = 0 \quad \forall x \in [0,L] \tag{3.2}$$

3.2.2 Spatial discretization

Weak formulation for a single element

The weak formulation of the problem defined by equation 3.1 with the boundary conditions given in equation 3.2 is obtained by multiplying the first one of them by a generic test function $u^*(x)$ following a double integration by parts. Particularly, if a conventional finite element approach is adopted, the domain $x \in [0,L]$ is subdivided into elements of length l^e and Hermitian polynomials are used both as test functions as well as interpolating functions. Subsequently, the integration by parts of 3.1 is carried out over each element. This technique is widely known and is treated extensively in a number of works, see for instance the monograph by Zienkievick or Bathe [23, 24].

Regarding the element shown in figure 3.3, the function $w(x,t)$ is approximated by a cubic polynomial using the four Hermitian polynomials $h_n(x)$, $(n = 1-4)$:

$$w(x^e,t) = \sum_{n=i}^{4} y_n^e(t) h_n^e(x^e) \tag{3.3}$$

where the physical meaning of the time-varying coefficients is the usual one, i.e. the transverse displacement and slope at the nodes:

$$y_1^e(t) = y_i(t), \quad y_2^e(t) = \theta_i(t),$$
$$y_3^e(t) = y_j(t), \quad y_4^e(t) = \theta_j(t)$$

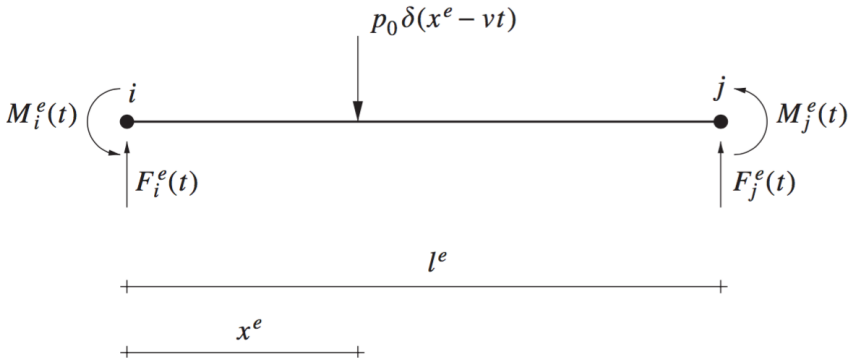

Figure 3.3: Positive nodal forces and moments in the linear element. Source: [1]

The approximate velocity and acceleration are obtained by differentiation of $w(x^e,t)$ with respect to time:

$$\dot{w}(x^e,t) = \sum_{n=i}^{4} \dot{y}_n^e(t) h_n^e(x^e), \quad \ddot{w}(x^e,t) = \sum_{n=i}^{4} \ddot{y}_n^e(t) h_n^e(x^e), \tag{3.4}$$

where overdot denote time derivatives. Using also the four Hermitian polynomials as test functions, and approximating the spatial variables by means of equations 3.3 and 3.4, weak form of equation 3.1 is obtaining integrating within the element. The moment-curvature relationship in Bernoulli-Euler beams and Dirac delta function identities have been applied to finally obtain:

$$\int_0^{l^e} m(x^e) \sum_{n=1}^{4} \left[\ddot{y}_n^e(t) h_n^e(x^e)\right] h_m^e(x^e) \mathrm{d}x^e + \int_0^{l^e} \sum_{n=1}^{4} \left[y_n^e(t) \frac{\mathrm{d}^2 h_n^e(x^e)}{\mathrm{d}(x^e)^2} \right] EI(x^e) \frac{\mathrm{d}^2 h_m^e(x^e)}{\mathrm{d}(x^e)^2} \mathrm{d}x^e$$
$$= F_j^e(t) h_m^e(l^e) + F_i^e(t) h_m^e(0) + M_j^e(t) \frac{\mathrm{d}h_m^e(x^e)}{\mathrm{d}x^e}|_{l^e} + M_i^e(t) \frac{\mathrm{d}h_m^e(x^e)}{\mathrm{d}x^e}|_0 - p_0 h_m^e(vt) \qquad (3.5)$$

with $m = 1, 2, 3, 4$. The variables $F_i^e(t), F_j^e(t)$ and $M_i^e(t), M_j^e(t)$ are forces and bending moments in nodes i and j of element e, whose sign criterion is shown in figure 3.3.

Matrix formulation for a single element

After evaluation of the integrals contained in equations 3.5, the solution can be expressed in matrix form as follows:

$$\begin{bmatrix} m_{11}^e & m_{12}^e & m_{13}^e & m_{14}^e \\ m_{21}^e & m_{22}^e & m_{23}^e & m_{24}^e \\ m_{31}^e & m_{32}^e & m_{33}^e & m_{34}^e \\ m_{41}^e & m_{42}^e & m_{43}^e & m_{44}^e \end{bmatrix} \begin{bmatrix} \ddot{y}_i(vt) \\ \ddot{\theta}_i(vt) \\ \ddot{y}_j(vt) \\ \ddot{\theta}_j(vt) \end{bmatrix} + \begin{bmatrix} k_{11}^e & k_{12}^e & k_{13}^e & k_{14}^e \\ k_{21}^e & k_{22}^e & k_{23}^e & k_{24}^e \\ k_{31}^e & k_{32}^e & k_{33}^e & k_{34}^e \\ k_{41}^e & k_{42}^e & k_{43}^e & k_{44}^e \end{bmatrix} \begin{bmatrix} y_i(vt) \\ \theta_i(vt) \\ y_j(vt) \\ \theta_j(vt) \end{bmatrix}$$
$$= \begin{bmatrix} F_i^e(vt) \\ M_i^e(vt) \\ F_j^e(vt) \\ M_j^e(vt) \end{bmatrix} - p_0 \begin{bmatrix} h_1^e(vt) \\ h_2^e(vt) \\ h_3^e(vt) \\ h_4^e(vt) \end{bmatrix}$$

which can also be rewritten in a more compact form as:

$$\mathbf{M}^e \ddot{\mathbf{y}}^e(t) + \mathbf{K}^e \mathbf{y}(t) = \mathbf{f}^e(t) - p_0 \mathbf{h}^e(vt) \qquad (3.6)$$

The elements of the matrices in equations 3.6 are given by:

$$m_{rs}^e = \int_0^{l^e} m(x^e) h_r^e(x^e) h_s^e(x^e) \mathrm{d}x^e,$$
$$k_{rs}^e = \int_0^{l^e} \frac{\mathrm{d}^2 h_r^e(x^e)}{\mathrm{d}(x^e)^2} EI(x^e) \frac{\mathrm{d}^2 h_s^e(x^e)}{\mathrm{d}(x^e)^2} \mathrm{d}x^e \qquad (3.7)$$

where r and s run from 1 to 4.

Assembled formulation

Assembling the element equations 3.6, the differential equation of motion of the finite element model of the beam is obtained:

$$\mathbf{M}\ddot{\mathbf{y}}(t) + \mathbf{K}\mathbf{y}(t) = -p_0\mathbf{h}(vt) \tag{3.8}$$

It can be seen, the load term is a vector with an analytic, polynomial expression for $t \in [x_i^e/v, x_j^e/v)$. In what follows it will be assumed that the load has moved to the next element when $t = x_j^e/v$. In order to solve equation 3.8 , the boundary conditions need to be prescribed. After applying the boundary conditions, the new reduced mass and stiffness matrices define the problem to be solved. For simplicity, in what follows the reduced matrices will be referred to using the same symbols as the non-reduced ones, and distinction will be made when it is necessary.

3.2.3 Semi-analytic solution

Solution of the equations of motion

Equation 3.8 is a matrix system of linear differential equations with constant coefficients and an analytical right-hand term. This equation can be solved through a change of basis given by the generalized eigenvalue problem described by:

$$(-\omega^2\mathbf{M} + \mathbf{K})\mathbf{y}(t) = 0 \;\Rightarrow\; \det\left(\mathbf{K} - \omega^2\mathbf{M}\right) = 0 \tag{3.9}$$

being ω the eigenvalue. Let $\mathbf{q}(t)$ be time-dependent modal amplitude vector, related to $\mathbf{y}(t)$ though the matrix $\mathbf{C}$:

$$\mathbf{y}(t) = \mathbf{C}\mathbf{q}(t) \tag{3.10}$$

where each column of $\mathbf{C}$ contains the corresponding eigenvector which are known as modes. Premultiplying 3.8 by $\mathbf{C}^T$ and changing from $\mathbf{y}(t)$ to $\mathbf{q}(t)$ it is obtain:

$$\mathbf{C}^T\mathbf{M}\ddot{\mathbf{q}}(t) + \mathbf{C}^T\mathbf{K}\mathbf{q}(t) = -p_0\mathbf{C}^T\mathbf{h}(vt) \tag{3.11}$$

The matrix product in the left-hand terms of equation 3.11 are both diagonal as a result of the orthogonality property of the modes. Therefore, 3.11 becomes:

$$\mathbf{M}_D\ddot{\mathbf{q}}(t) + \mathbf{K}_D\mathbf{q}(t) = -p_0\mathbf{C}^T\mathbf{h}(vt) \tag{3.12}$$

The problem can now be solved for a unitary load $p_0 = 0$ and, assuming linear behaviour of the system, the solution for a different load can be computed multiplying the unitary solution by the actual value of p_0. Premultiplying equation 3.12 by the inverse of the diagonal mass matrix, and letting $p_0 = 1$:

$$\ddot{\mathbf{q}}(t) + \mathbf{M}_D^{-1}\mathbf{K}_D\mathbf{q}(t) = \mathbf{G}\mathbf{h}(vt) \tag{3.13}$$

where:

$$\mathbf{G} = -\mathbf{M}_D^{-1}\mathbf{C}^T \tag{3.14}$$

Solution for each mode

With the exception of the time intervals when the load is applied in one element having a restrained degree of freedom, the elements of vector $\mathbf{h}(vt)$ in the right-hand term of equation 3.13 are zero in all but four rows. These four rows correspond precisely to the degrees of freedom of the i and j nodes belonging to the element e where the moving load is applied. Thereby, the differential equation for the nth mode can be expressed as:

$$\ddot{q}_n(t) + \omega_n^2 q_n(t) = \sum_{m=1}^{4} G_{nm}^e h_m^e(vt) \tag{3.15}$$

At this point it is possible to include the damping effects by means of a modal damping ratio ζ_n. In this way equation 3.15 transforms into:

$$\ddot{q}_n(t) + 2\zeta_n\omega_n\dot{q}_n(t) + \omega_n^2 q_n(t) = \sum_{m=1}^{4} G_{nm}^e h_m^e(vt) \tag{3.16}$$

The solution of equation 3.16 can be obtained in closed-form, but the analytic expression needs to be defined piecewise for every different time interval $[x_i^e/v, x_j^e/v]$. Every time the load crosses from one element to the next one, the closed-form expression of the solution is redefined. Consider that the load is moving in element e, having initial and final nodes i and j. In order to solve equation 3.16, a change of the origin of the time variable is introduced. Let t be the time relative to the instant when the load passes over the initial node $i \quad \tau = t - x_i^e/v$. Then, the initial conditions can be specified in the form:

$$q_n(\tau = 0) = q_n^0, \quad \dot{q}_n(\tau = 0) = \dot{q}_n^0 \tag{3.17}$$

with $\tau \in [0, l^e/v)$.

The solution can now be expressed as the sum of the solution of the homogeneous equation plus a particular solution:

$$q_n(\tau) = q_n^h(\tau) + q_n^p(\tau)$$

During the time interval in which the load traverses the structure, the particular and homogeneous solutions will have to be added, giving rise to the forced vibration and free vibration contributions, respectively. Conversely, after the load has reached the last node of the beam only the contribution of the homogeneous solution will remain.

The mathematical expressions of the homogeneous solution is:

$$q_n^h(\tau) = e^{-\zeta_n \omega_n \tau} \left(A_n \cos(\omega_n^d \tau) + B_n \sin(\omega_n^d \tau) \right) \tag{3.18}$$

with $\omega_n^d = \omega_n \sqrt{1 - \zeta_n^2}$.

On the other hand, the particular solution can be expressed by:

$$q_n^p(\tau) = \alpha_n^{(0)} + \alpha_n^{(1)} vt + \alpha_n^{(2)} (vt)^2 + \alpha_n^{(3)} (vt)^3 \tag{3.19}$$

where coefficients $\alpha_n^{(i)}$ $(i = 0 - 3)$ can be obtained solving the equations below:

$$\begin{aligned}
\alpha_n^{(0)} &= v^3 \alpha_n^{(01)} + v^2 \alpha_n^{(02)} + v \alpha_n^{(03)} + \alpha_n^{(04)} \\
\alpha_n^{(2)} &= v^2 \alpha_n^{(11)} + v \alpha_n^{(12)} + \alpha_n^{(13)} \\
\alpha_n^{(3)} &= v \alpha_n^{(21)} + \alpha_n^{(22)} \\
\alpha_n^{(4)} &= \alpha_n^{(31)}
\end{aligned} \tag{3.20}$$

In the above expressions, the dependence of the speed v has been isolated using the following 10 coefficients:

$$\begin{aligned}
\alpha_n^{(01)} &= -\frac{24\zeta_n(2(\zeta_n)^2-1)(2G_{n1}^e-2G_{n3}^e+(G_{n2}^e+G_{n4}^e)l^e)}{(l^e)^3(\omega_n)^5}\\
\alpha_n^{(02)} &= -\frac{2(4\zeta_n^2-1)(3G_{n1}^e-3G_{n3}^e+(2G_{n2}^e+G_{n4}^e)l^e)}{(l^e)^2(\omega_n)^4}\\
\alpha_n^{(03)} &= -\frac{2G_{n2}^e\zeta_n}{(\omega_n)^3}\\
\alpha_n^{(04)} &= \frac{G_{n1}^e}{(\omega_n)^2}\\
\alpha_n^{(11)} &= \frac{6(4(\zeta_n)^2-1)(2G_{n1}^e-2G_{n3}^e+(G_{n2}^e+G_{n4}^e)l^e)}{(l^e)^3(\omega_n)^4}\\
\alpha_n^{(12)} &= \frac{4\zeta_n(3G_{n1}^e-3G_{n3}^e+(2G_{n2}^e+G_{n4}^e)l^e)}{(l^e)^2(\omega_n)^3}\\
\alpha_n^{(13)} &= \frac{G_{n2}^e}{(\omega_n)^2}\\
\alpha_n^{(21)} &= -\frac{6\zeta_n(2G_{n1}^e-2G_{n3}^e+(G_{n2}^e+G_{n4}^e)l^e)}{(l^e)^3(\omega_n)^3}\\
\alpha_n^{(22)} &= -\frac{3G_{n1}^e-3G_{n3}^e+(2G_{n2}^e+G_{n4}^e)l^e}{(l^e)^2(\omega_n)^2}\\
\alpha_n^{(31)} &= \frac{2G_{n1}^e-2G_{n3}^e+(G_{n2}^e+G_{n4}^e)l^e}{(l^e)^3(\omega_n)^2}
\end{aligned} \tag{3.21}$$

At this point, it should be emphasized that this ten coefficients together with the speed of the moving load define the particular solution. Furthermore, coefficients of equations 3.21 can be computed and stored initially for the entire mesh.

On the other hand, coefficients of the homogeneous solution (equation 3.18) are obtained from the initial conditions(equations 3.17) as follows:

$$\begin{aligned}
A_n &= q_n^0 - \alpha_n^{(0)}\\
B_n &= \frac{\dot{q}_n^0 + \zeta_n\omega_n A_n - \alpha_n^{(1)}v}{\omega_n^d}
\end{aligned} \tag{3.22}$$

The complete closed-form solution is built piecewise from a set of analytic functions, one per element. For the initial time,$t = 0$, at-rest conditions are normally imposed:

$$q_n(\tau=0)=0, \quad \dot{q}_n(\tau=0)=0$$

For the following elements, the initial conditions for element $e + 1$ are given by the end values of element e.

Solution for a set of moving loads

For a set or series of concentrated loads moving at a constant speed v, which represent in more realistic way HSR bridges problems, the solution can be obtained by superposition.

3.3 Generalization of the formulation

Semi-analytic solution is expressed trough the sum of homogeneous solution (equation 3.18) plus a particular solution (3.19) per each mode n. As it can be seen in this equations, parameters that define this solutions such as C_n, ω_n or G_n are obtained in the modal analysis. In fact the temporal solution is defined analytically. In any moment geometrical restriction, such as section type or inertia, are imposed. Unlike, geometrical information is indirectly include in the modal solution. Therefore, equation 3.1 can be replaced by the general one that follows:

$$\mathcal{L}\{u(\bar{x},t), v(\bar{x},t), w(\bar{x},t)\} = -p_0\delta(s - vt) \tag{3.23}$$

being $\mathcal{L}$ a differential operator and s the curvilinear coordinate of the load line.

A general governing equation 3.23 can be solve using separation variables technique and the system can then be decoupled by modal analysis. The only imposition observed is that load line must be class C^1 so that the spatial discretization by the Hermite polynomials allows a smooth transition avoiding the existence of discontinuities that could introduce fictive acceleration peaks.

To sum up, the methodology presented herein follow the next scheme for a moving load problem with any geometry:

- Computation of ω_n, $\mathbf{C}$ and $\mathbf{G}$ using any FE software by modal analysis.
- Estimation of the ten coefficients α_n.
- Carrying out the temporal integration of the solution using the semi-analytic algorithm.
- Evaluating the solution (accelerations and displacements) in post-processing points previously selected.

As it can be seen, the overall procedure depends only on the spatial discretization and the time step selected for evaluating the solution without the need of any integration step.

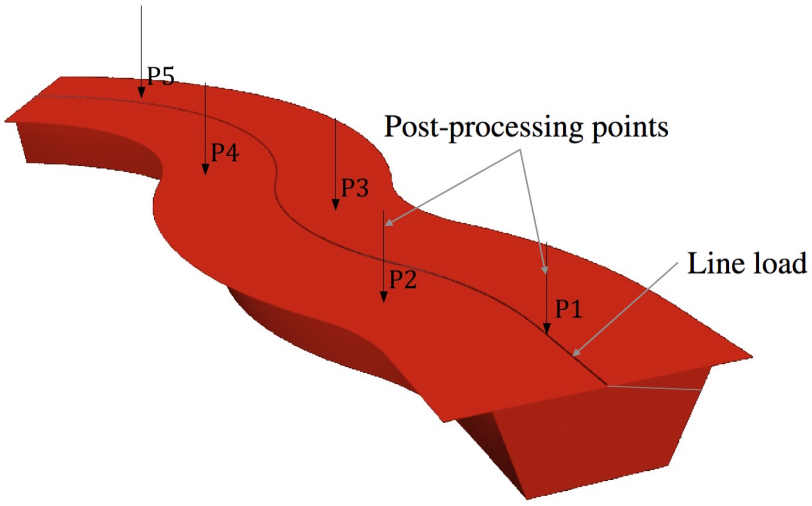

Figure 3.4: Line load and post-processing points scheme.

3.4 Advantages of the method

This semi-analytic method have been successfully tested by the authors in some different geometries. Paper [1] is focused on 1D structures, specifically non-uniform Bernoulli-Euler beams. This document presents four different examples.

On one side, paper sections 5.1 to 5.3 show three different comparisons of the results obtained using the semi-analytic method and a classic time-stepping procedure: the linear acceleration version of the Newmark method. The aim is to validate the new approach. The three analyzed structures are: a three-span continuous stepped beam under a single moving load, a three-span continuous haunched beam also under a single moving load and the same three-span continuous haunched beam under a train of moving loads.

On the other side, paper section 5.4 presents a practical application of the semi-analytic method to the dynamic analysis of a three-span bridge according to Eurocode 1 [4].

Another reference is [25], which was part of the Eurodyn 2005 program (International Conference on Structural Dynamics). In this case, the paper is focus on the semi-analytic solution for Kirchhoff plates traversed by moving loads.

Furthermore, this methodology has been used in the design of a bridge on the high speed line Córdoba-Málaga close to the town of Santa Ana (Antequera). After the accomplishment of a laborious dynamic study using the semi-analytic algorithm, a bow-string bridge was finally decided. The process is explained in [19].

In view of the excellent testing results, the semi-analytic solution seems to be a very proper approach to dynamic problems. The main advantages of the method are:

- Apart from numerical roundoff errors, the only approximation introduced in the procedure comes from the spatial discretization of the structure, which is inherent to any Finite Element model. Any geometry is permitted.
- The time-dependent modal equations are solved in closed-form, and therefore, the method is highly accurate and robust, circumventing the main disadvantages of time-stepping schemes.
- A time step is required in order to evaluate the solution and obtain a representation of the response time- history. Nevertheless, the equations of motion

are integrated analytically, and therefore the response computed at any given time instant is not affected by the size of the step. This fact directly affects to computational cost, since step-by-step methods require much more calculation in order to obtain a solution as accurate as semi-analytic method. So, the method has proved to be computationally efficient.

- The solution is obtained in terms of 10 coefficients per element and per mode. These coefficients are independent of the speed of the moving loads, and therefore, need not be recalculated if an analysis for different values of speed is to be carried out.

- This saving of time makes it particularly useful for the design of actual bridges, allowing structural engineers to evaluate and compare the performance of different alternatives quickly and efficiently. It becomes a practical and realistic tool to evaluate bridges applying IAPF-07, whose main requirements are:

  a) Considering more than 10 different trains.

  b) Circulation speeds from 20 km/h to 400 km/h approximately, with speed step of 1 km/h to analyze the complete range of accelerations. Thus it would be analyzed around 380 circulation speeds.

  c) At least three load cases are analyzed, considering three different values of the ballast weight.

  Accordingly to this estimation, in a general dynamic problem it must be done over $10 \times 380 \times 3 = 11400$ algorithm iterations. So the reduction of the process time gets by the semi-analytic method is very valuable.

CHAPTER

4

Case study: Almonte river viaduct

4.1 Introduction

Madrid-Lisbon high-speed rail line is a proposed high speed line between the Iberian capitals. It forms part of the Trans-European high-speed rail network, which is one of the Trans-European transport networks (TEN-T), and was defined by the Council Directive 96/48/EC of 23 July 1996.

In 2012 the project was cancelled officially on the Portuguese side due to not being financially viable. Despite that fact, Spanish high speed infrastructure manager *ADIF Alta Velocidad* is continuing work. In 2016 the European Regional Development Fund (FRDF), gave Spain €205.1m towards the €312.1m needed for the track between Navalmoral de la Mata and Mérida, Spain. Two capital structures have been built as a part of this HSR line: the viaduct over the Tajo river and the viaduct over the Almonte river, both concrete arch bridges solutions located nearby the Alcántara reservoir.

The Almonte bridge (see figure 4.1) have been selected to perform a dynamic

study of it, because of its singularity. The aim of this study is to analyze the specific behavior of HSR arch bridges, such as arch-deck low-frequency modes, torsion modes derived from the off-centered moving load over the deck, continuos and maximum deflections and accelerations induced by high speed trains,...

To accomplish this objective the semi-analytic methodology is used in order to reduce computational time and thus be able to perform the analysis of different models. In total, five different models of the viaduct have been developed, considering soil-structure interaction in one of them.

Figure 4.1: The viaduct over the Almonte river in construction phase. Source: FCC Construccion, S.A. official website (`http://www.ciudadfcc.com/`).

4.2 About viaduct over the Almonte river

The Almonte river viaduct is part of the HSR line Madrid-Extremadura. Trains crossing the bridge may reach speeds of up to 350 kilometers per hour. It is located in the Alcántara Reservoir in the western region of Cáceres. The viaduct has a main arch span of 384 meters, and a total length of 998 meters and at its apex the arch rises 70 meters above the river. Its main arch span makes this project the largest HSR arch in the world and the largest railway bridge in Spain. The approach spans of the bridge range from 36 to 45 meters. The bridge uses reinforced and prestressed high-strength concrete. It was designed by Guillermo Capellán, Héctor Beade, Javier Martínez and Emilio Merino from Spanish Engineering firm *Arenas&Asociados*. To sum up, in table 4.1 are included main characteristics of the Almonte river viaduct.

Table 4.1: Data sheet of the Almonte river bridge.

Location	Alcántara Reservoir, Cáceres, Spain
Design engineers	Arenas&Asociados
Owner	Adif Alta Velocidad
Contractor	FCC Constructions&Conduril Engineering
Completed	2016
Main span	384 m
Total length	996 m
Structural system	Deck arch bridge pointed

The mechanism for taking the longitudinal forces from trains braking is the fixed point located on top of the key of the arch, as it can be seen in figure 4.2. At the center of the bridge there is a 42 m long fixed point connecting the arch and the deck. Horizontal loads due to the train braking are transferred through the fixed point from the deck to the arch and then into the foundation. All of the horizontal forces present are transmitted to the fixed point, as the columns are connected to the deck with elastomeric bearings, allowing the deck to move longitudinally with respect to the columns.

The simplest initial design for the supporting piers of this bridge would use a rectangular cross-section with constant width along the height of the column. However, by making two simple adjustments to the conventional pier shape, the designers were able to lessen the wind effects. First, the cross-section of each column is octagonal, which leads to better airflow around the columns, mitigating lateral wind forces. Additionally, the columns narrow towards the top. This design is efficient because piers are massive in the places where bending moments are higher.

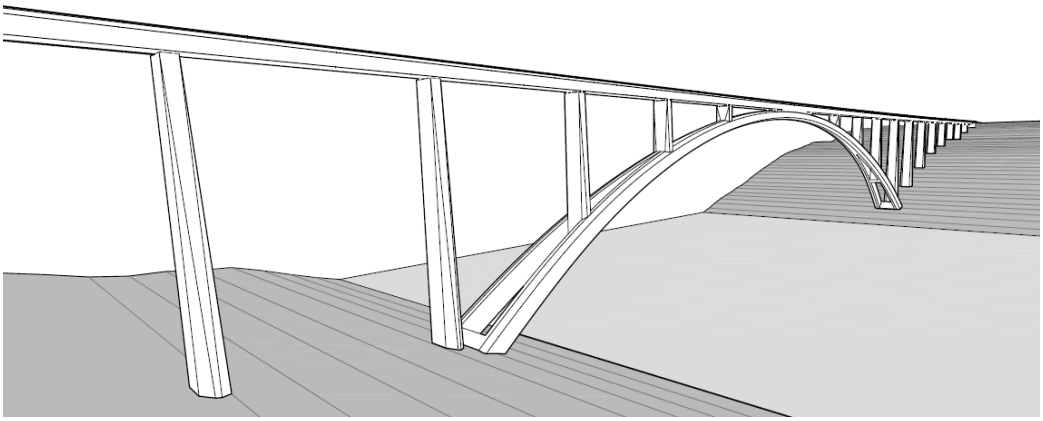

Figure 4.2: Perspective drawing of the Almonte bridge. Source: construction blueprints.

Like the columns, the cross-section of the arch varies throughout the structure trying to be exclusively under compressive stresses. The arch section widens towards the foundation (see figure 4.3). The arch splits into two legs which provide the lateral support necessary to resist wind and other transversal loads acting on the bridge.

The bridge has a continuous prestressed concrete box girder deck with constant cross-section with almost $3\,\text{m}$ depth and a total width of $14\,\text{m}$ (figure 4.5). The bridge deck over the arch is composed by 7 spans $42\,\text{m}$ long supported by the arch. Access spans are $45\,\text{m}$ long, except first and last one which are $36\,\text{m}$ long. Each span was provided with one diaphragm at each end.

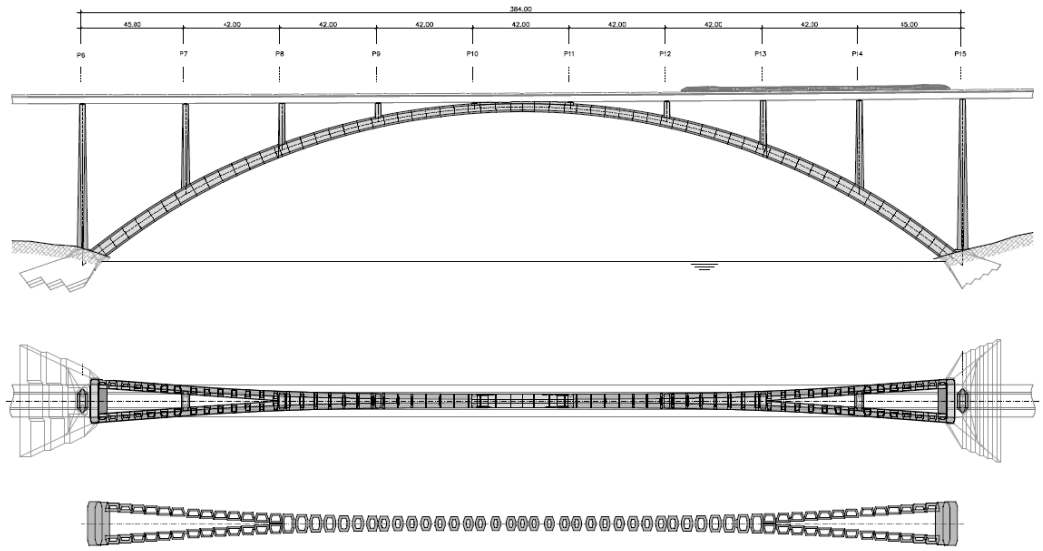

Figure 4.3: Main view, bird's-eye view and arch cross-sections of the Almonte bridge. Source: construction blueprints.

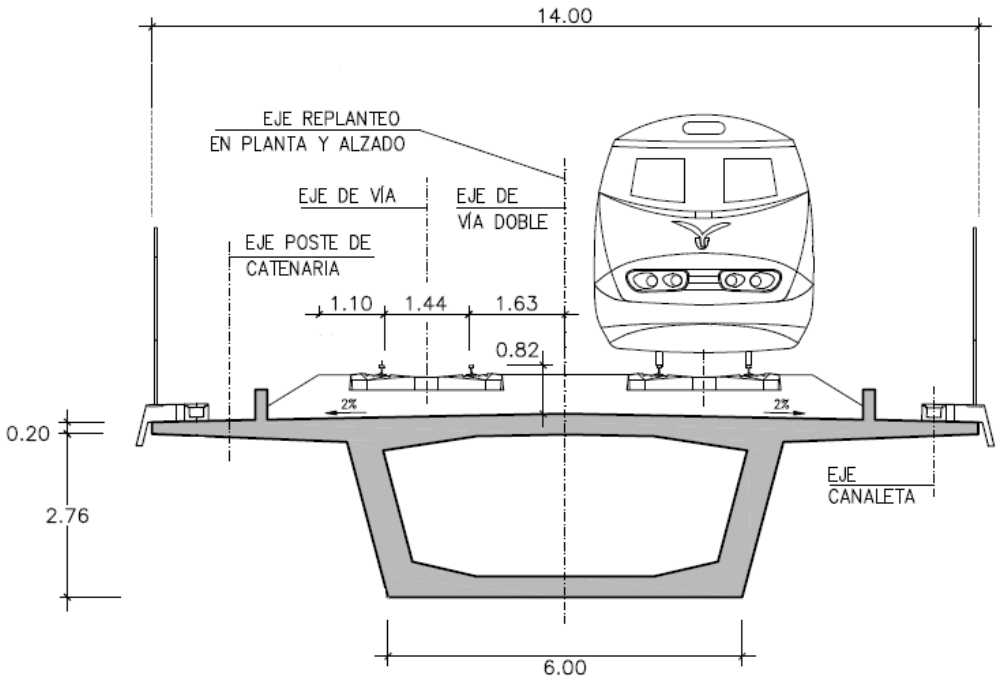

Figure 4.4: Deck cross-section type. Source: construction blueprints.

Construction on the Almonte River Viaduct began in 2011 and was managed by *Adif*. The contractor was *FCC Construction&Conduril Engeneering*, a temporary consortium of this two companies. A system of movable formwork on the piers was used to construct the deck. The arch was constructed using a cantilever method with temporary cables attached to the piers and to temporary steel towers.

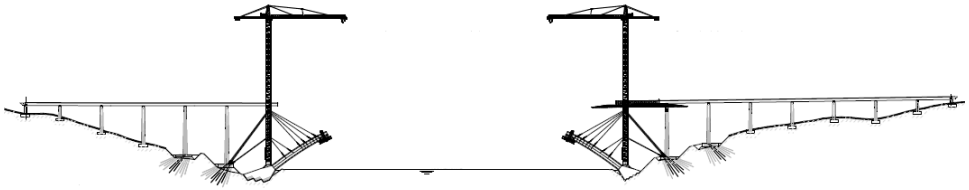

(a) Phase 1: arch construction by cantilever method.

(b) Phase 2: deck construction using movable formwork.

Figure 4.5: Main construction phases of the viaduct. Source: construction blueprints.

4.3 Numerical models

The first step to perform a time-domain dynamic analysis using semi-analytic method is to develop a numerical model to obtain natural frequencies and modes of the structure. The most extended method in bridge engineering to develop numerical models is the Finite Element Method (FEM). Using a FE free software as a tool, several numerical models of the Almonte river viaduct have been developed. This models are:

- Model 1: *Isolated arch using 1D elements*

  In this model only the main span is represented. That includes the arch, and pies and deck over it. All the model is made with linear elements.

- Model 2: *Complete viaduct using 1D elements*

This is Model 1 including access spans and abutments. The model is also made with linear elements.

- Model 3: *Isolated arch using 2D elements*

  Only the main span is represented like it occurs in Model 1, but in this case the deck is modeled by shell elements.

- Model 4: *Complete viaduct using 2D elements*

  It is similar to model 2 except for the deck, which is modeled by 2D elements.

- Model 5: *Isolated arch using 2D elements and considering soil-structure interaction*

  This is Model 3 with mass matrix and stiffness matrix located in the arch foundation to represents more realistically the behaviour of the structure, including soil-structure interaction.

Models with 1D elements (Models 1 and 2) are simpler so the are easier to develop. However situations such as a eccentric load or deck torsion modes can not be represented with them. Actually this models have been developed as a reference to compare the results obtain with 2D elements models.

On the other hand, the aim of developing an isolated arch model is to prove if this simplify model can represent appropriately the behaviour of the whole structure. If so, computational time can be reduced because the model is not so heavy than the complete one.

Finally Model 5 has been implemented to analyze how soil-structure interaction can affect the dynamic response of an structure and if it is a good practice to include this features on design models.

The five models are represented in figure 4.6 and details of them are described below.

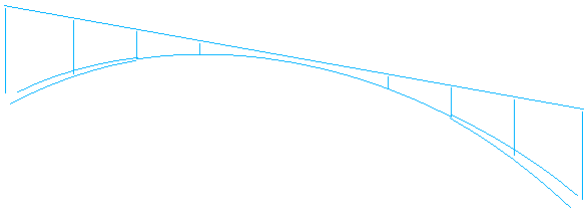

(a) Model 1.

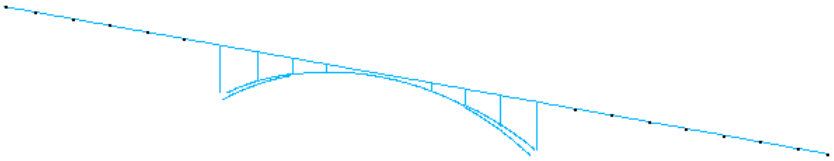

(b) Model 2.

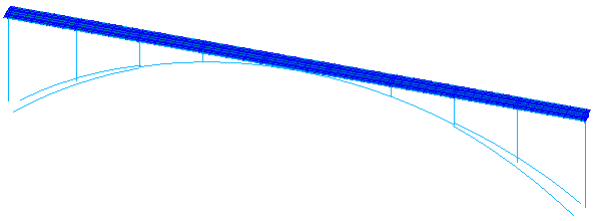

(c) Model 3.

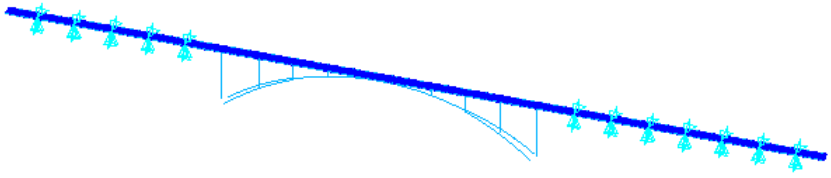

(d) Model 4.

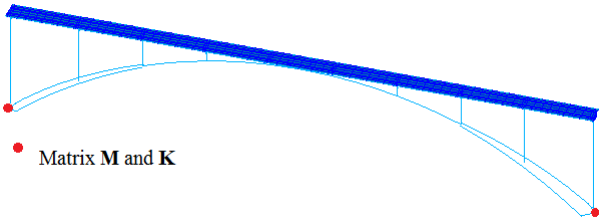

(e) Model 5.

Figure 4.6: Models of the viaduct over the Almonte river.

4.3.1 Geometry and finite element mesh

The geometry of the model have been obtain from the construction blueprints of the viaduct, politely provided by the contractor.

Arch

The main element of the viaduct, the arch, have been modeled by two nodes beam elements (1D or linear elements) in all models. In order to represent the variable cross-section of the arch, sections between piers have been divided into three and appropriate properties of the middle cross-sections have been introduced manually. The mesh size has been set to 1 m.

The connection between arch and deck (fixed point) are modeled as a rigid constrain between nodes. This union is plot in figure 4.7 in pink color.

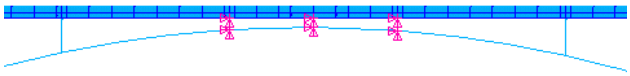

Figure 4.7: Model of fixed point at the key of the arch.

Piers

The piers of the access spans don't have been modeled directly. Instead, they have been replace by boundary conditions.

Nevertheless, the piers over the arch have been also modeled by two nodes beam elements. In this case, a preintegrated square hollow cross-section with linear variation has been introduce. The mesh size has also been set to 1 m. The

connection between arch and piers is also rigid ant it is shown in pink color in figure 4.8. Moreover, the cap of this piers have been modeled by rigid beams forming a 'V' shape, whose ends would coincide with the points where bearings are placed (see figure 4.11).

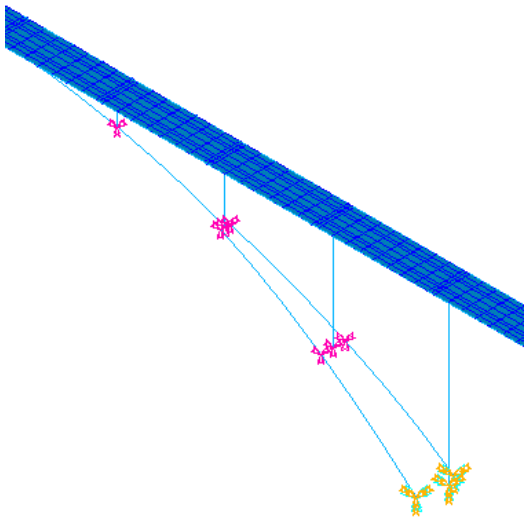

Figure 4.8: Model of connection between piers and double arch.

Deck

Two versions of the deck have been developed.

The *first* of them uses two nodes beam elements to represent the girder. Properties of a hollow box cross-section have been set in all spans sections. Also at each span end properties of the full box cross-section have been introduced to represents the presence of diaphragms.

The *second* one uses four nodes shell elements (2D elements) to form the shape of the cross-section, which is divided in four parts: the top flange that supports the track structure, the two webs, the bottom flange and diaphragms.

- Flanges:

  At the same time the top flange is divide in two different parts: the central part of constant thickness with added mass due to track structure and the cantilever verge of variable thickness without added mass. The value of the added mass is obtain from data in table 4.4.

  The bottom flange is modeled by shell elements of constant thickness without added mass.

- Webs:

  The beam cross-section to be modeled with shells is a typical example of in-plane bending-dominated problems. In this kind of problems, reduced integration (the most used one) would require refined meshes. For example, some geometries require several elements through the thickness to get an accurate solution. In order to avoid such a refined mesh, full integration is employed. However, bilinear elements, when fully integrated, are too stiff in in-plane bending. In this cases the method of incompatible modes is usually employed to enhance the accuracy.

  The webs of the box girder in the Almonte river represent an in-plane bending-dominated problem. Therefore, full integration with incompatible modes is implemented in the shell elements of the webs and thus an unrefined mesh is enough.

- Diaphragms:

  They are modeled using shell elements of constant thickness of $1.25\,\mathrm{m}$ at the ends of each span, with a gap. It is shown in figure 4.11.

Figure 4.9 displays the shape of flanges and webs. The part of the top flange in which it is assumed an added mass because of the track, elements are dark blue. Also a beam at the edge of the top flange (violet element) is considered to model the effect of the fencing and to avoid unrealistic flapping modes of high frequency in modal analysis performance.

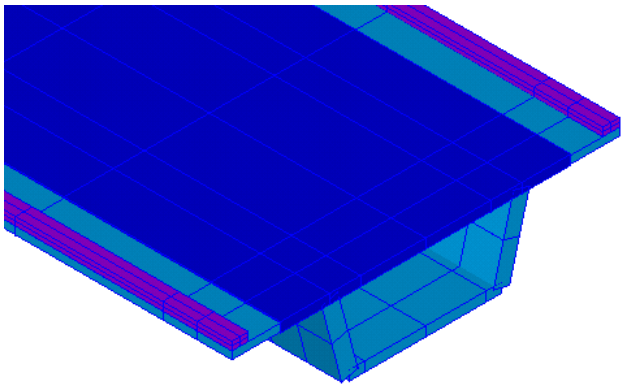

Figure 4.9: Model with elements 2D of the deck.

Bearing and abutments

Connection between deck and piers is bearing supported. There are two different types of guided POT bearings in each pier cap: type PU and type PL. The same support system is placed on abutments, so that train braking loads are only supported by the fixed point at the center of the arch, where deck and arch meet. The bearings have the next characteristics:

PU
- Allows longitudinal displacement.
- Constraints transversal displacement.
- Bears horizontal transversal loads.

PL
- Allows longitudinal and transversal displacement.
- Does not resist any horizontal load (except friction).

(a) Type PU (b) Type PL

Figure 4.10: Guided POT bearing scheme.

In models with 1D elements forming the deck, only one point of the deck is supported, so the most restrictive POT bearing (PU type) is defined at this node. In this sense, it is defined a constraint equation relating different degrees of freedom to model this connections between pier caps and deck (see figure 4.11). On the other hand, in the access spans, bearings are modeled by degree-of-freedom constraints at corresponding deck nodes.

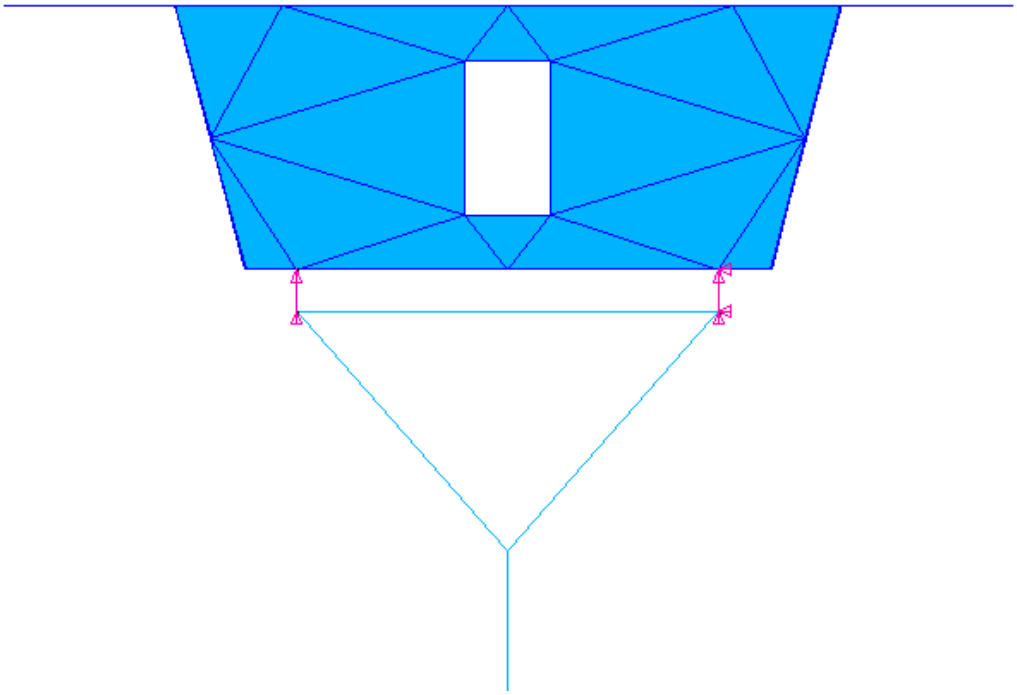

Figure 4.11: Deck cross-section type. Source: construction blueprints.

Foundation

In actual viaduct, piers number 6 and 15 and the two legs of the arch are underpinned in the same mass concrete block at each river side. It has been developed two different models of this foundation. The first model is that which do not consider soil-structure interaction. In this case, the ends of this elements have all degrees-of-freedom constrained.

On the other hand, there is a model which includes soil-structure interaction. In this case the ends of this elements are defined as a rigid region. Furthermore there is defined a node in the center of mass of the concrete block connected with the previous rigid region. The soil-structure interaction is thus modeled with a mass matrix and a stiffness matrix located at this node.

The *mass matrix* is a diagonal matrix containing concentrated mass components in coordinate directions and rotary inertias about the coordinate axes. To compute this values, a model of the foundation have been plot in a CAD software to obtain the volume (V) and the rotary inertias of the mass concrete block ($\tilde{I}_{xx}, \tilde{I}_{yy}, \tilde{I}_{zz}$). Considering a concrete density of $\rho = 2500\,\text{kg/m}^3$, the mass components ($M_x, M_y, M_z$) and dimensionally correct rotary inertias (I_{xx}, I_{yy}, I_{zz}) can be computed to express the mass matrix below:

$$\mathbf{M} = \begin{pmatrix} M_x & & & & & \\ & M_y & & & \underline{0} & \\ & & M_z & & & \\ & & & I_{xx} & & \\ & \underline{0} & & & I_{yy} & \\ & & & & & I_{zz} \end{pmatrix} \tag{4.1}$$

Mass components in coordinate directions has been considered to be the same, i. e.:

$$M_x = M_y = M_z = \rho \cdot V \tag{4.2}$$

And dimensionally correct rotary inertias can be obtain as:

$$I_{ii} = \rho \cdot \tilde{I}_{ii} \tag{4.3}$$

where $i = x, y, z$.

Stiffness matrix represents the foundation behaviour due to soil-structure interaction. The definition of the stiffness matrix is not so immediate because the response of the soil foundation depends on the deformed shape of the structure and this response in turn depends on the load case. Scientific community have been studied this problem since the end of the past century, trying to obtain impedance

functions not only for static loads but also for dynamic problems. There exist both analytical and numerical methods to estimate dynamic impedance functions associated with a rigid but massless foundation [26, 27, 28]. In [29] G. Gazetas presents a complete review of formulas and charts for impedances of surfaces and embedded foundations.

The general problem statement consider an arbitrary basement shape foundation on an homogeneous or even multilayer half-space. For a particular harmonic excitation, the dynamic impedance is defined as the ratio between force (or moment) and the resulting steady-state displacement (or rotation) at the centroid of the base of the massless foundation. For example, the vertical impedance is obtain as the solution of the problem shown in figure 4.12 and it can be expressed as:

$$S_y = \frac{R_y(t)}{U_y(t)} \tag{4.4}$$

where $R_y(t)$ and $U_y(t)$ are the harmonic vertical load and the harmonic vertical displacement of the foundation respectively. This two functions have the next expressions:

$$R_y(t) = R_y e^(i\omega t) \tag{4.5}$$

$$U_y(t) = U_y e^(i\omega t) \tag{4.6}$$

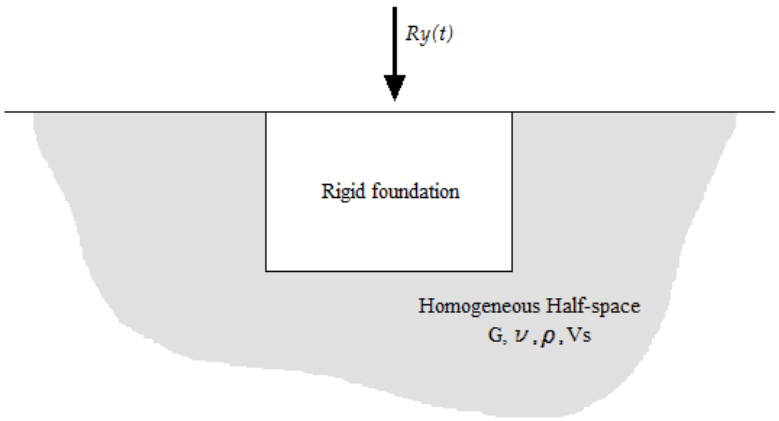

Figure 4.12: Vertical impedance problem statement.

Similarly the following impedances are defined:

S_z : lateral swaying impedance.

S_x: longitudinal swaying impedance.

S_{θ_x} : rocking impedance for rotation about x axis.

S_{θ_z} : rocking impedance for rotation about z axis.

S_{θ_y}: torsional impedance for rotation about vertical axis.

Furthermore, mainly in embedded foundations horizontal forces along principal axes induce rotational oscillations (in addition to translational); hence, two more 'cross-coupling' horizontal-rotational impedances are considered: $S_{x-\theta_z}$ and $S_{z-theta_x}$.

Because of the presence of radiation and material damping, R and U are generally out of phase and the impedances can be expressed in complex notation as follows:

$$S = K_{real} + iK_{im} = \hat{K} + i\omega C \tag{4.7}$$

in which both $\hat{K}$ and C depend on frequency ω. This two components, the real one and the imaginary, can be interpreted as:

$\hat{K} \rightarrow$ 'Dynamic stiffness': it represents the stiffness of the foundation for dynamic loads.

$C \rightarrow$ 'Damping coefficient': it reflects the radiation and material damping generated in the system due to energy carried by waves spreading away from the foundation and energy dissipated in the soil by hysteretic phenomena.

Equation 4.7 suggests that the soil-structure interaction can be modeled, for each frequency, as a set of springs (stiffness matrix $\mathbf{K}$) and dampers (damping matrix $\mathbf{C}$) with the characteristic values of $\hat{K}$ and C computed for each direction. So finally the stiffness matrix that represents the soil-structure interaction in the

FE model can be expressed in the cartesian axes (with vertical axis y) placed at the centroid of the foundation as follows:

$$\mathbf{K} = \begin{pmatrix} K_x & 0 & 0 & 0 & 0 & K_{x-\theta_z} \\ 0 & K_y & 0 & 0 & 0 & 0 \\ 0 & 0 & K_z & K_{z-\theta_x} & 0 & 0 \\ 0 & 0 & K_{y-\theta_x} & k_{\theta_x} & 0 & 0 \\ 0 & 0 & 0 & 0 & K_{\theta_y} & 0 \\ K_{x-\theta_z} & 0 & 0 & 0 & 0 & K_{\theta_z} \end{pmatrix} \tag{4.8}$$

In order to include SSI in the FE model of the Almonte bridge, the Boundary Elements Method (BEM) is used to obtain the solution of a embedded foundation in half-space subject to a particular harmonic excitation. Particularly, the approach of Guzina, Pak and Martínez-Castro [30] of the singular boundary elements are use to solve the dynamic problems. As it is refers on the previous paper, it is advisable use non-dimensional parameters of the problem in order to obtain an accurate solution. Thus, in this case study a rectangular foundation of a representative dimension and a medium limestone soil foundation are considered. The main characteristics of the limestone is shown in table 4.2. Furthermore, the frequency considered in the problem is for the first vertical mode of the bridge (ω_1). As it can see, it is a recurrent problem. First, a dynamic load of frequency ω_1 obtain with a modal analysis of the FE model without SSI is considerer to obtain the stiffness matrix expressed by equation 4.8. Secondly, a brand-new modal analysis is developed for the FE model including SSI and the load frequency ω_1 is updated.

Table 4.2: Geotechnical parameters of the foundation limestone.

E (MPa)	80
ν	0.3
G (MPa)	30
ρ (kg/m^3)	2200
v_s (m/s)	115

On the other hand, also the damping effect of the foundation is considered in the dynamic analysis of the viaduct. The BEM code also provides the imaginary components of the impedances K_{im}, so the damping ratio for each mode i can be

obtained as the sum of the ratio of each two foundations:

$$\zeta_i = \frac{\Phi_i^T \mathbf{C} \Phi_i}{2\omega_i}|_{C1} + \frac{\Phi_i^T \mathbf{C} \Phi_i}{2\omega_i}|_{C2} \tag{4.9}$$

where

ζ_i: damping ration for mode i.

Φ_i: modal displacements and rotation at the foundation for mode i.

ω_i: natural frequency of mode i.

$\mathbf{C}$: damping matrix computed using BEM. The components of the matrix can be obtain as $C = K_{im}/\omega_1$.

4.3.2 Materials and dead loads

The only material present in the viaduct is the concrete. There are considered several concrete types to form the bridge:

- HP-40/B/20/IIa $\rightarrow$ in access spans deck.
- HP-60/B/20/IIa $\rightarrow$ in spans over the arch desk.
- HA-80/AC/12/IIa $\rightarrow$ in the arch.
- HA-40/B/20/IIa $\rightarrow$ in piers (except piers 6 and 15).
- HA-50/B/12/IIa $\rightarrow$ in piers 6 and 15.

For all this materials, there value of density considered is $\rho = 2500\,\text{kg7m}^3$ and the poisson coefficient $\nu = 0.2$. The value of the elastic modulus depends on the characteristic strength of the concrete. To asses this value, the formula of article 39.6 of the EHE-08 [31] is used. The values obtained are present in table 4.3.

Table 4.3: Concrete parameters.

Concrete	f_{ck} (MPa)	E_{cm} (GPa)
HP-40 or HA-40	40	31
HA-500	50	31
HP-60	60	35
HA-80	80	38

On the other hand, the lineal weight of the elements of the track are list below in table 4.4.

Table 4.4: Dead load due to track elements.

Ballast	13437 kg/m
Rails and railway sleepers	1280 kg/m
Ballast boards	500 kg/m
Fencing	900 kg/m

4.4 Dynamic analysis in time domain

Here most remarkable aspects of the dynamic performance are point out.

4.4.1 Traffic loads on bridges

The dynamic analysis has been done following the instructions of the IAPF-07. In particular, analysis type defined in appendix B of the instruction is applied, so the ten trains defined in appendix C.1 (Universal Dynamic Train) are considered.

The design speed of the line is $v_d = 350$ km/h, so train speeds from 20 km/h to 420 km/h ($1.2v_d$) have been considered in the calculation.

4.4.2 Serviceability limit state requirements

Main checks stablished by the instruction IAPF-07 are:

- Maximum deflection to check the serviceability limit state (SLE).
- Maximum vertical acceleration to assure comfort and ballast stability.
- Maximum rotation at the abutments.

The points of the deck in which previous magnitudes are compute are:

- Deflection:

  In spans over the arch, in centre span cross-sections and quarter span cross-sections, at the rail axis.

  In access spans there is any post-processing point.

- Vertical acceleration:

  In spans over the arch, in centre span cross-sections and quarter span cross-sections, at three points for each section: at longitudinal axis of the deck, at right edge of the ballast and at left edge of the ballast.

  In access spans, in centre span cross-sections, at right edge of the ballast.

4.4.3 Settings of the modal analysis

A modal analysis determines the vibration characteristics, natural frequencies and mode shapes, of a structure. It can also serve, as in the case here, as a starting point for a more detail dynamic analysis such a transient dynamic analysis.

The mode extraction method use in this work is the so-called *Block Lanczos*. The Block Lanczos eigenvalue solver uses the Lanczos algorithm where the Lanczos

recursion is performed with a block of vectors. In the computation, consistent mass matrix is considered and modes with a value of frequency lower than 30 Hz are obtain.

4.4.4 Settings of the semi-analytic method

Basis of the semi-analytic method have been developed in Chapter 3, so here only the main parameters of the method are exposed.

Modes and natural frequencies are obtain from a modal analysis of a FE model of the bridge. For the modal superposition analysis, modes whose frequency is lower than 30 Hz are considered, as it was said previously.

Time step chosen to evaluate the vibration time solution of the viaduct is one tenth of the lowest period of vibration. Thus been the highest frequency 30 Hz, the time step is about $\Delta t = 3e^{-3}$ s.

Free vibrations in the bridge are computed for over a total time of 6 times the period of the fundamental mode, which is considerate enough time to obtain the maximum oscillations of the structure.

Damping ratio due to material is considered the same for all of modes, with a value of 2%. In model with SSI, additional damping ratios defined by equation 4.9 are included.

CHAPTER

5

Results

5.1 Introduction

The main aim of this research is to develop a methodology for dynamic analysis of HSR bridges based on the semi-analytic method. In addition, another goal is to get the suitable one FE model for this kind of problems by analyzing different options. In order to achieve these objectives there have been developed several dynamic analysis of the five FE models.

Particularly, a previous and needed modal analysis of all models is performed. The results of this study is presented in next section.

Afterward some dynamic analysis have been performed to compare different models. First of all, some temporal series have been obtain in order to analyze bridge behaviour. Three cases have been considered:

- The passage of an isolated moving load at a speed of 50 km/h.

- The passage of the train A1 defined in appended C.1 of the IAPF-07, at a speed of 50 km/h.

- The passage of the train A1 at a speed of 300 km/h.

Lastly, for models with 2D elements deck the complete dynamic analysis of the Universal Dynamic Train defined in the IAPF-07 has been performed. This analysis include the passage of the ten trains so-called A1 to A10 at a speed from 20 km/h to 420 km/h, with a speed step of 1 km/h.

To sum up all the performances carried out are shown in table 5.1.

Table 5.1: Dynamic performances of different FE models.

	Model1	Model2	Model3	Model4	Model5
Modal analysis	*	*	*	*	*
Isolated moving load	*		*		
Train A1 at 50 km/h	*		*		
Train A1 at 300 km/h	*		*	*	
Universal Dynamic Train	*			*	

5.2 Modal analysis

There have been developed five modal analysis, one for each different model. The main results of the first five vertical bending arch modes are shown below. As it can be seen in table 5.2 and figure 5.1, frequencies of the vertical bending modes and mode shapes of different models mainly coincide. This is good news because it means that five FE models show the same behaviour and probably they represent the viaduct vibrations characteristics.

Table 5.2: Comparative of the first five frequencies for models 1-5.

	Natural frequency (Hz)				
	Model 1	Mode 2	Model 3	Model 4	Model 5
Mode 1	0.3037	0.2861	0.3069	0.2889	0.3058
Mode 2	0.6153	0.6190	0.6167	0.6199	0.5975
Mode 3	0.9616	0.9456	0.9768	0.9553	0.9644
Mode 4	1.2725	1.2714	1.2836	1.2819	0.9846
Mode 5	2.0329	1.8701	2.0699	2.1076	1.9805
Modes < 30 Hz	193	297	335	681	339

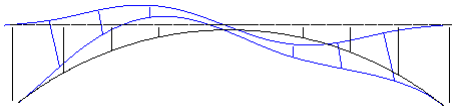

(a) Model 1

(b) Model 2

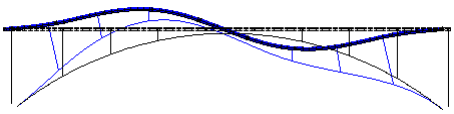

(c) Model 3

(d) Model 4

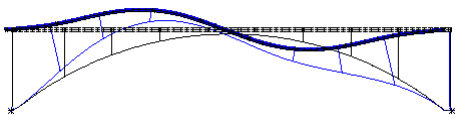

(e) Model 5

Figure 5.1: First vertical bending arch modes.

The total number of modes under < 30 Hz increase according to the complexity of the model. Models with finite elements 2D present a greater number of modes. Anyway, in all modal analysis first modes are longitudinal bending modes of the arch as it can be seen in figure 5.2. In models with access spans, also the arch response governs the problem. After this arch modes, the longitudinal bending modes of the deck appear, as well as the torsional and lateral bending coupled modes. In models with elements 2D, the last modes are bending modes of the edge flanges.

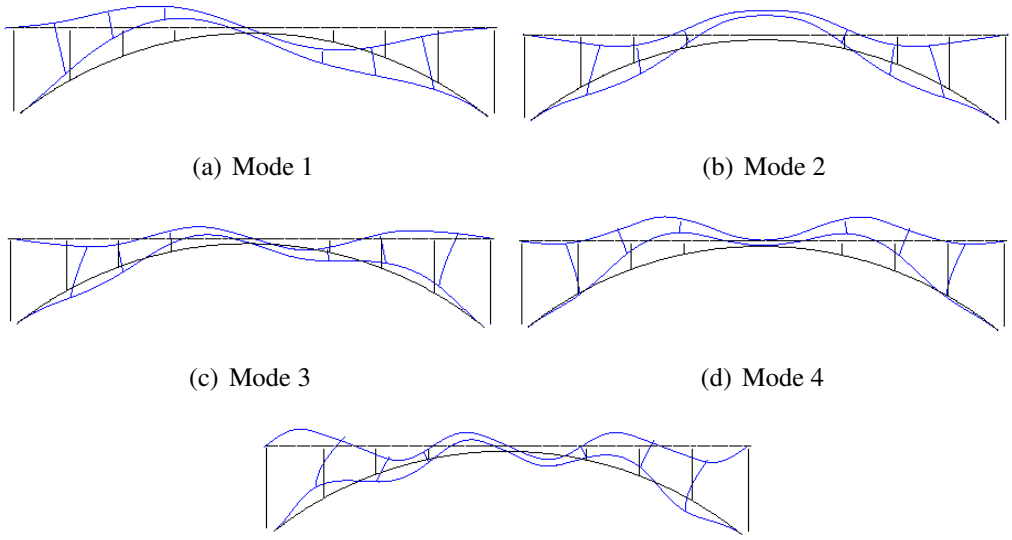

(a) Mode 1 (b) Mode 2

(c) Mode 3 (d) Mode 4

(e) Mode 5

Figure 5.2: Mode shapes of the first five vertical bending modes of model 1.

5.3 1D model *Vs* 2D model

This section presents the temporal series obtain in the analysis of two of the five models: model 1 and model 3. In both models only the arch is represented. Model 1 deck is represented with beam elements whereas model 3 deck is formed with shell elements. Therefore, the aim of this section is compare 1D and 2D models.

There have been developed three different analysis:

- The passage of a simple moving load at a speed of 50 km/h.
- The passage of the train A1 at a speed of 50 km/h.
- The passage of the train A1 at a speed of 300 km/h.

In three cases the load is applied over the longitudinal axis of the bridge, that means at the central point of the deck cross-section. This is because in model 1 the deck is represented as a beam, so it is difficult to apply a eccentric load in this situation.

It is also necessary to mention that in this three analysis, only the contribution of the first vibration mode is considered. The reason for doing this is to validate the models carefully and to assure that the first mode, which as an important effect on the response, is correct.

Next three figures show the temporal solution in terms of acceleration and displacement.

Two first load cases considered are quasi-static and the figures 5.3 and 5.4 represent time response at central point of the bridge. This point is the most rigid one due to the deck-arch connection. For all this, the displacement solution shown in figures 5.3b and 5.4b is almost not oscillating.

On the other hand, the third load case represent a dynamic problem due to the high speed imposed. In this case, the response represented in figure 5.5 is calculated at central point of the span placed next the keystone of the arch. As it can be seen in figure 5.5b, now the displacement response is oscillating and it has a great value.

In the light of the results it can be said that both responses of 1D and 2D models are very similar.

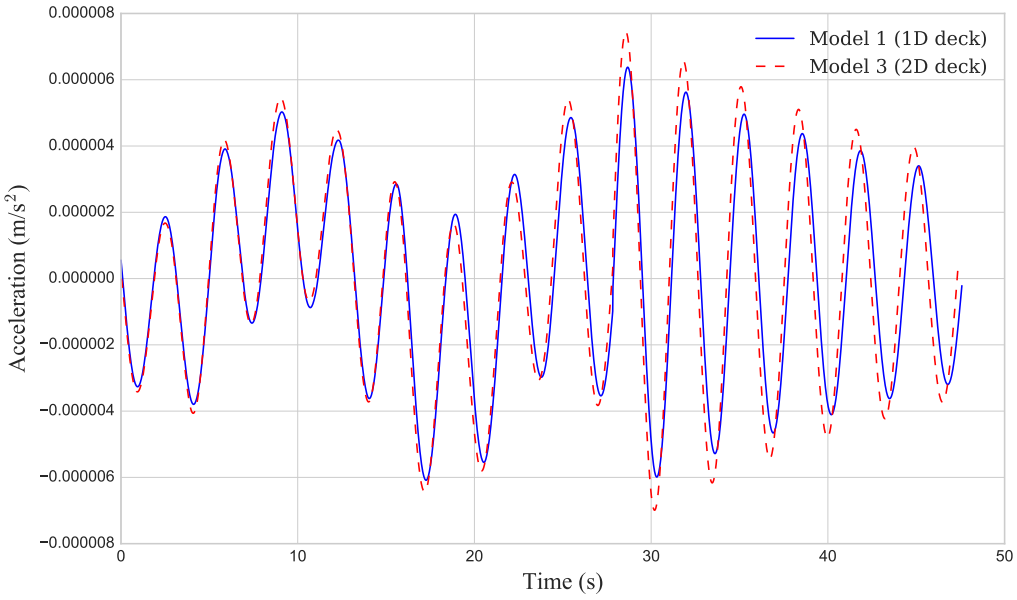

(a) Temporal series of acceleration.

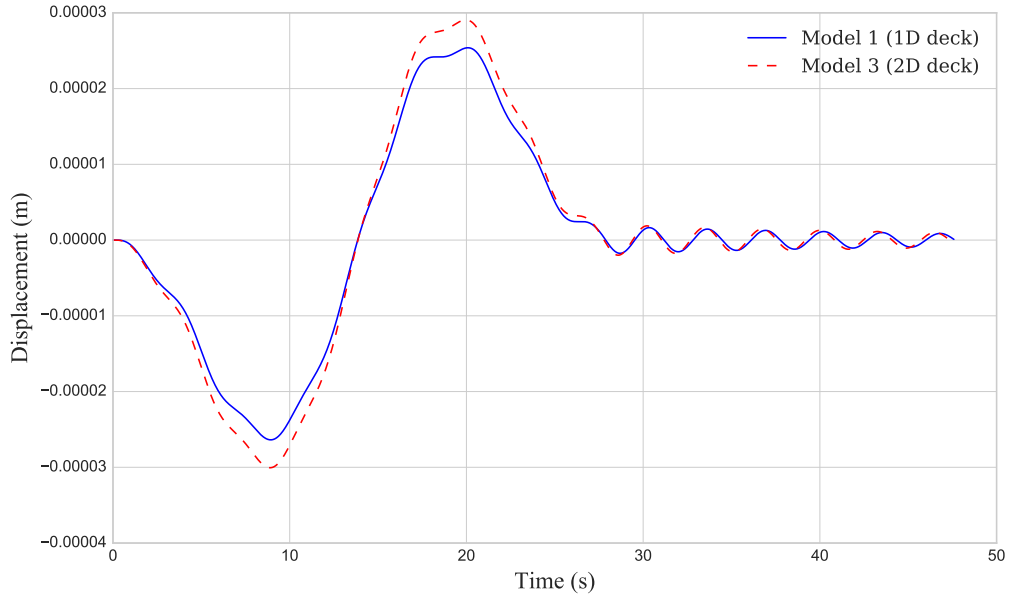

(b) Temporal series of displacement.

Figure 5.3: Results at center point of the arch due to the passage of an isolated moving load.

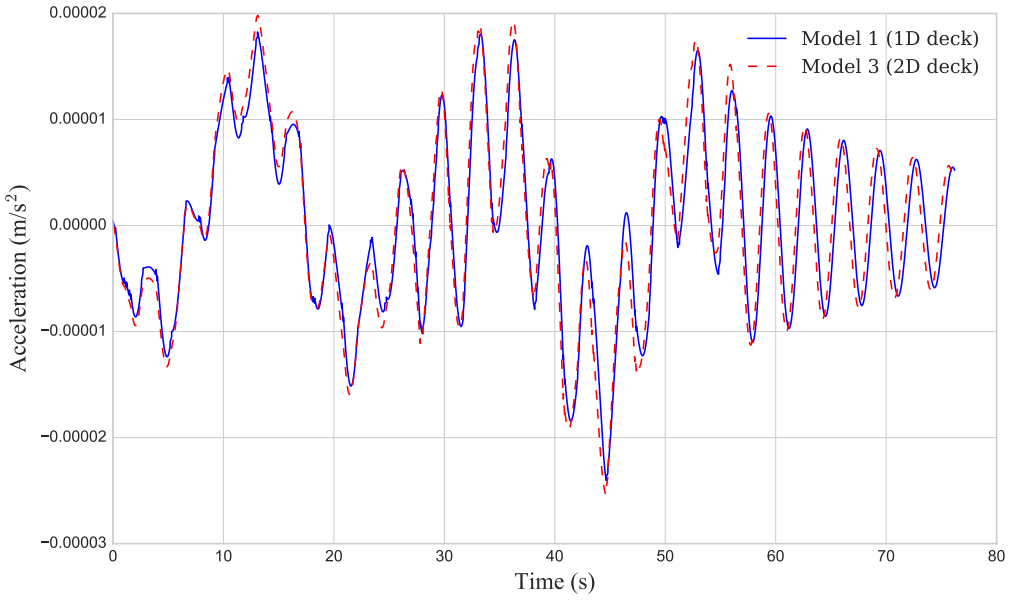

(a) Temporal series of acceleration.

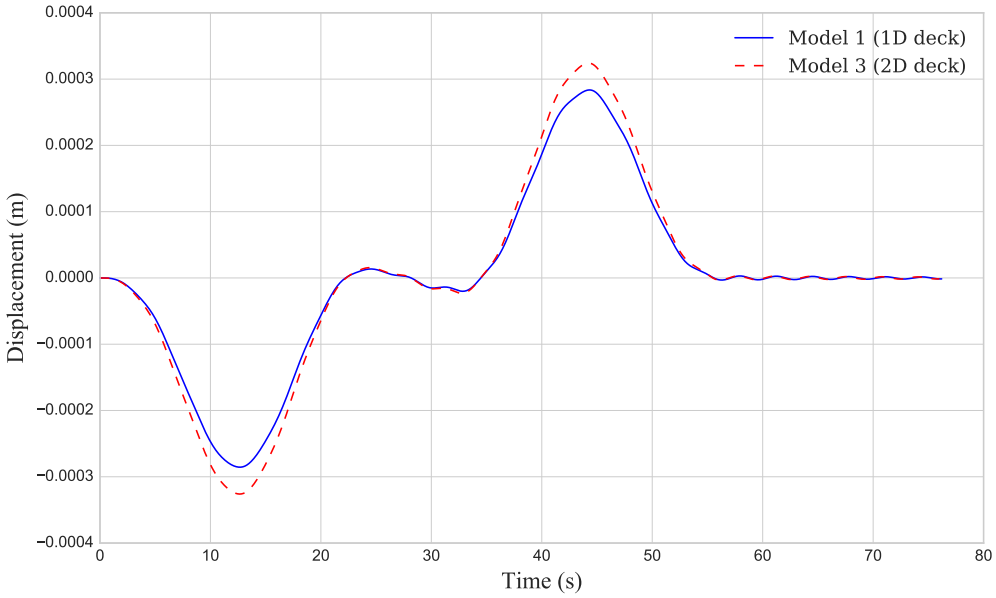

(b) Temporal series of displacement.

Figure 5.4: Results at center point of the arch due to train A1 passing at 50 km/h.

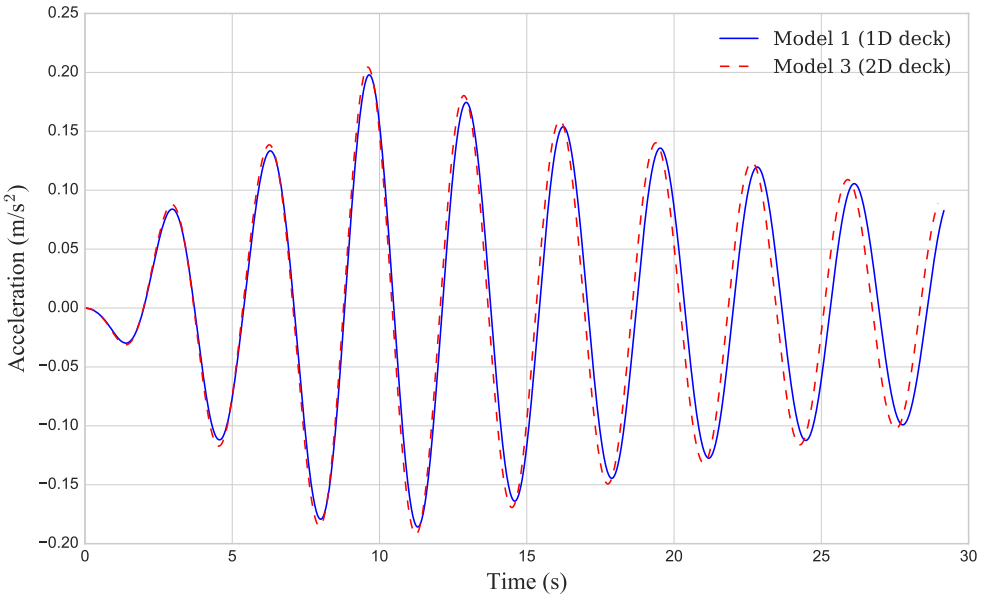

(a) Temporal series of acceleration.

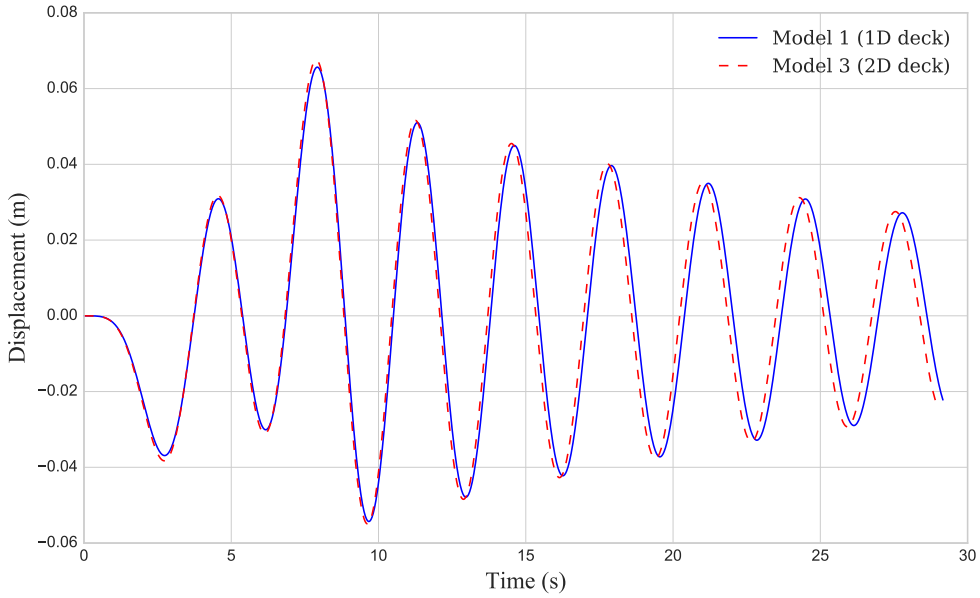

(b) Temporal series of displacement.

Figure 5.5: Results at the span before the central one due to train A1 passing at 300 km/h .

5.4 Arch model Vs Complete model

This section presents the temporal series and the maximum vibration response obtain in the analysis of two of the five models: model 3 and model 4. In this case both models have a deck formed with 2D elements. Then the difference between them lies in the geometry: model 3 is a model of the isolated arch and model 4 represents the complete viaduct. Therefore, the aim of this section is compare a simplify model of the bridge with the complete one.

There have been developed two different analysis:

- The passage of the train A1 at a speed of 300 km/h.
- The passage of the Universal Dynamic Train (ten trains so-called A1 to A10) at a speed from 20 km/h to 420 km/h, with a speed step of 1 km/h.

In this two cases the load is applied over the right rail, in order to represent real train loads. Also it is remarkable to say that in these analysis the contribution of all vibration modes with a frequency lower than 30 Hz are considered.

The temporal solution represented in figures 5.6, 5.7, 5.8 and 5.9 for models 3 and 4 are not overlapped because of the time variable do not coincide in both analysis. This is because in model 4 the load travels through the bridge's access spans but this is not the case in model 3. Anyway, at the light of this plots it can be said that responses of simplified and complete models are almost equal both in terms of values and shape.

Figures 5.6 and 5.7 represent the temporal solution at the keystone of the arch. Comparing these graphs with figures 5.8 and 5.9 it can be observe the effect of the fixed point at the center or the bridge.

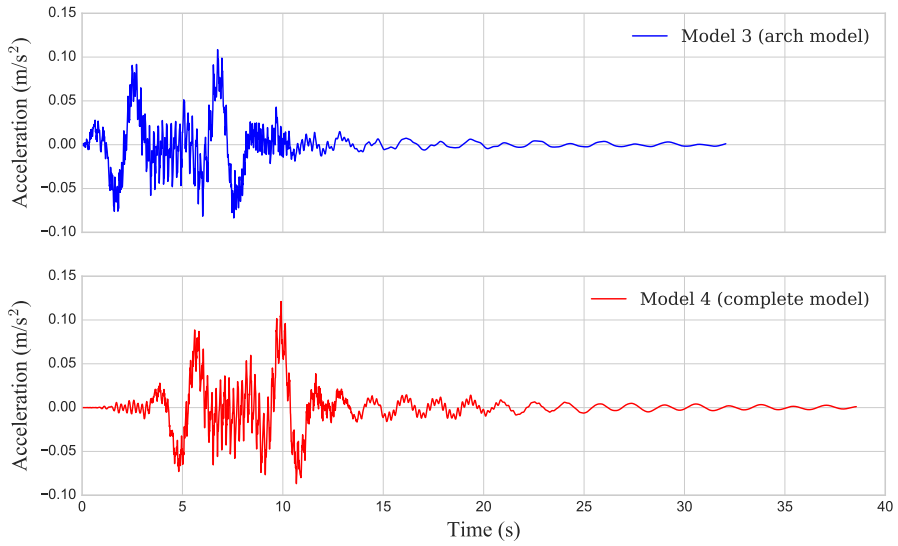

Figure 5.6: Acceleration at center point of the arch due to the passage of train A1 at 300 km/h.

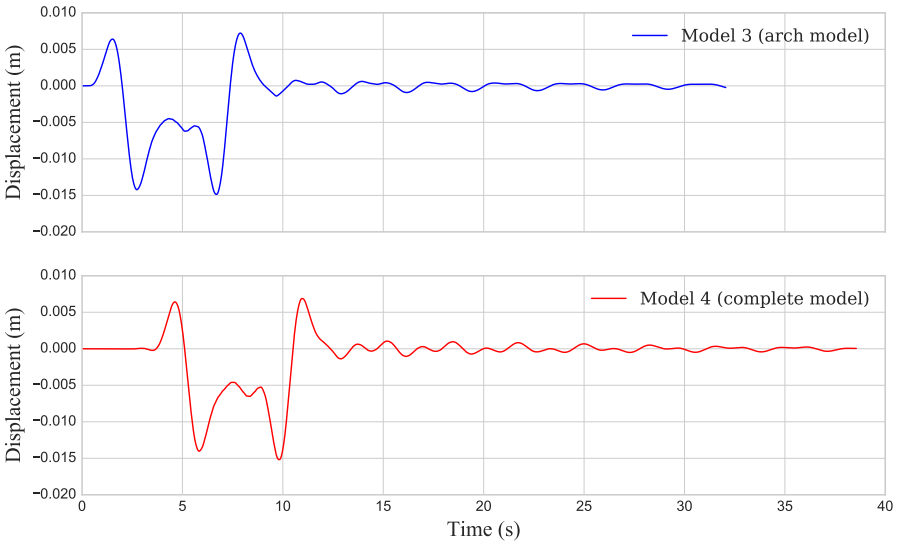

Figure 5.7: Displacement at center point of the arch due to the passage of train A1 at 300 km/h.

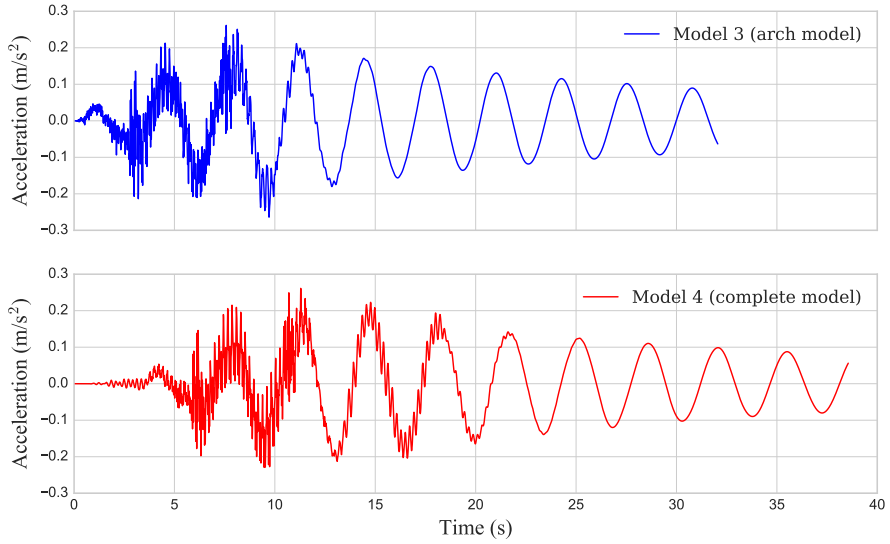

Figure 5.8: Acceleration at span after the central one due to the passage of train A1 at 300 km/h.

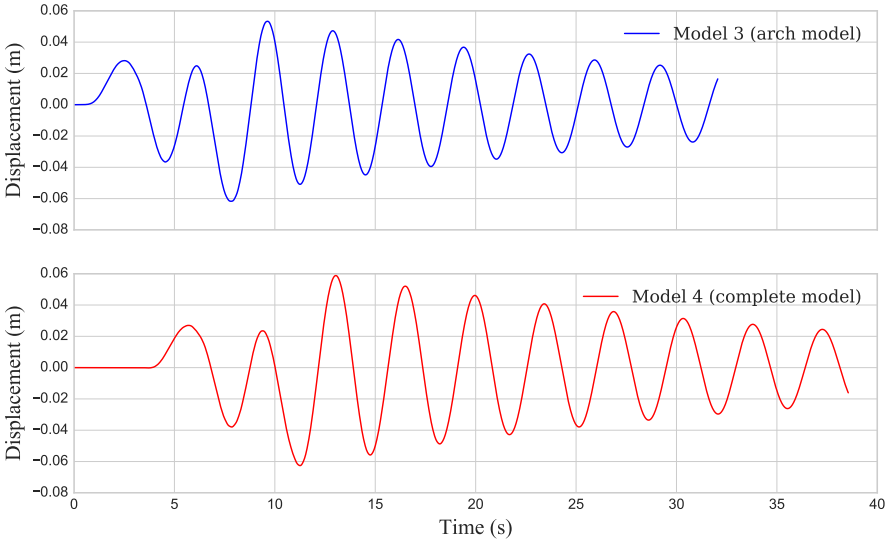

Figure 5.9: Displacement at span after the central one due to the passage of train A1 at 300 km/h.

On the other hand, the complete dynamic analysis have been developed. In this analysis, the enveloped curves of displacement and acceleration are obtain at each post-processing point. These enveloped curves represent the maximum acceleration (or displacement) due to the passage of a specific train as a function of the train speed. Analyzing all this data, the maximum maximorum values of acceleration and displacement are obtain. This results are resumed in tables 5.3 and 5.4 and the corresponding enveloped curves are shown in figures 5.10, 5.12,5.11 and 5.13.

Analyzing acceleration data of model 4 (the complete model) the maximum value of acceleration obtain is $1.5624\,\mathrm{m/s^2}$ at first post-processing point due to the passage of the train A3. This solution should be taken with caution because it can be the result of the impact of the train load when entering the bridge. So, the next maximum acceleration is obtain for train A2 at span number 12, the one situated next to the keystone. The location of this point of maximum acceleration, and also the train, coincide in the analysis of both models 3 and 4. The value of the maximum acceleration is near in both cases: $1.2986\,\mathrm{m/s^2}$ and $1.1426\,\mathrm{m/s^2}$ respectively.

Table 5.3: Maximum vertical acceleration information.

	Model 3	Model 4
Value	$1.2986\,\mathrm{m/s^2}$	$1.1426\,\mathrm{m/s^2}$
Train	A2	A2
Post-procesing Point	span 12	span 12

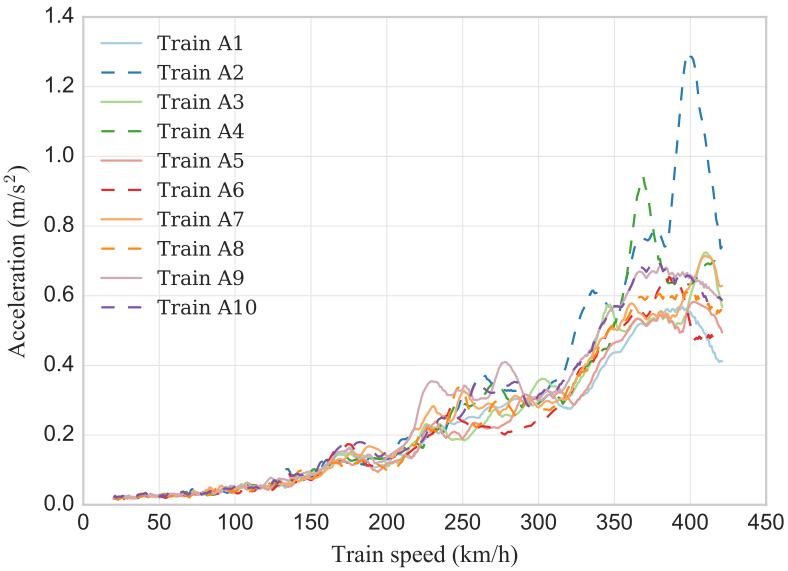

Figure 5.10: Acceleration envelope curves at post-processing point on span 12 for model 3.

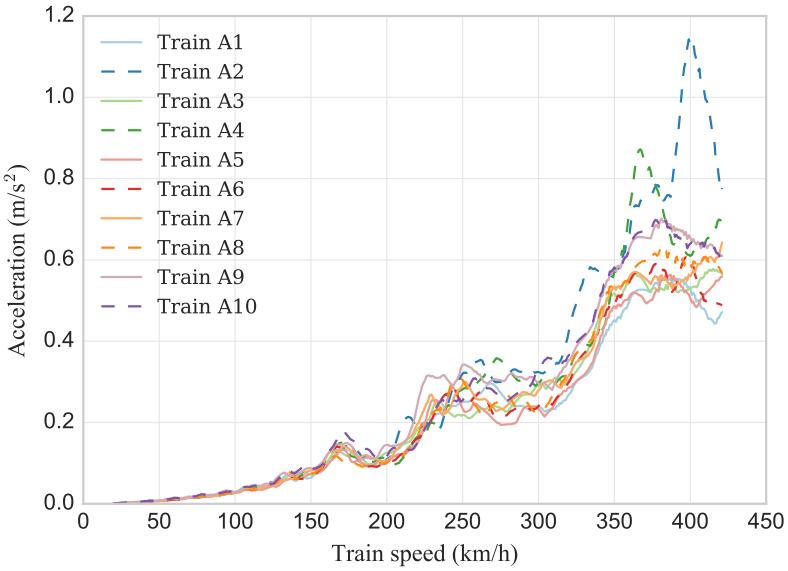

Figure 5.11: Acceleration envelope curves at post-processing point on span 12 for model 4.

In the case of the maximum displacement, the value is even closer: 9.69 cm for model 3 and 9.55 cm for model 4. This value is a bit high in relation to the restrictions of the IAPF-07. However, the value of elastic modulus of concrete considered in the FE models is prudent for a HP-80 MPa. Probably even for a more restrictive value of the concrete properties the value of the maximum displacement would be lower. Anyway the value obtain in both analysis is almost the same, for the same train and in the same location.

Table 5.4: Maximum vertical displacement information.

	Model 3	Model 4
Value	9.69 cm	9.55 cm
Train	A2	A2
Post-procesing Point	span 13	span 13

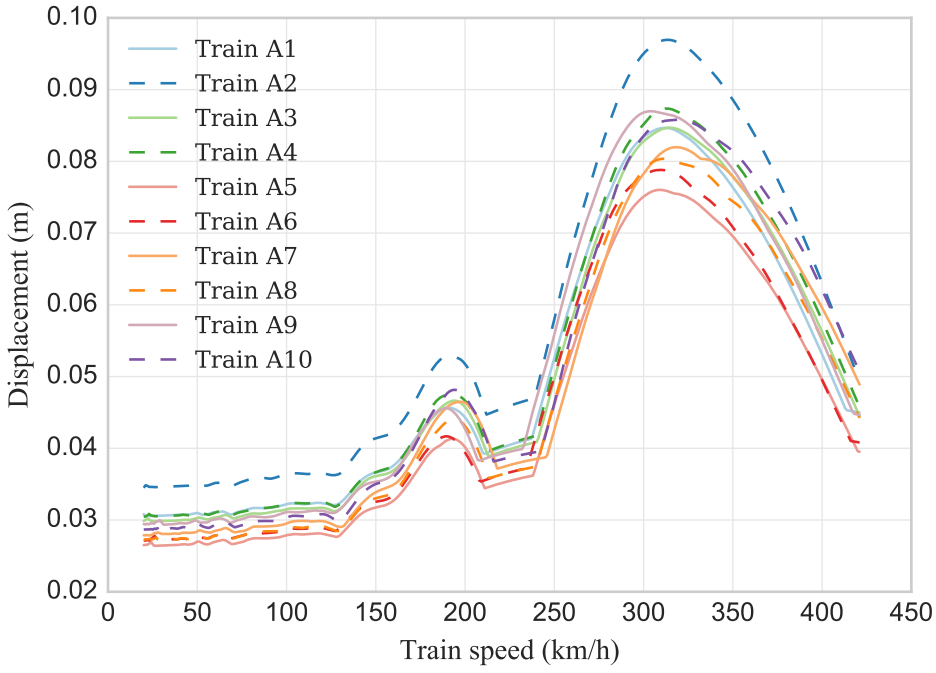

Figure 5.12: Displacement envelope curves at post-processing point on span 12 for model 3.

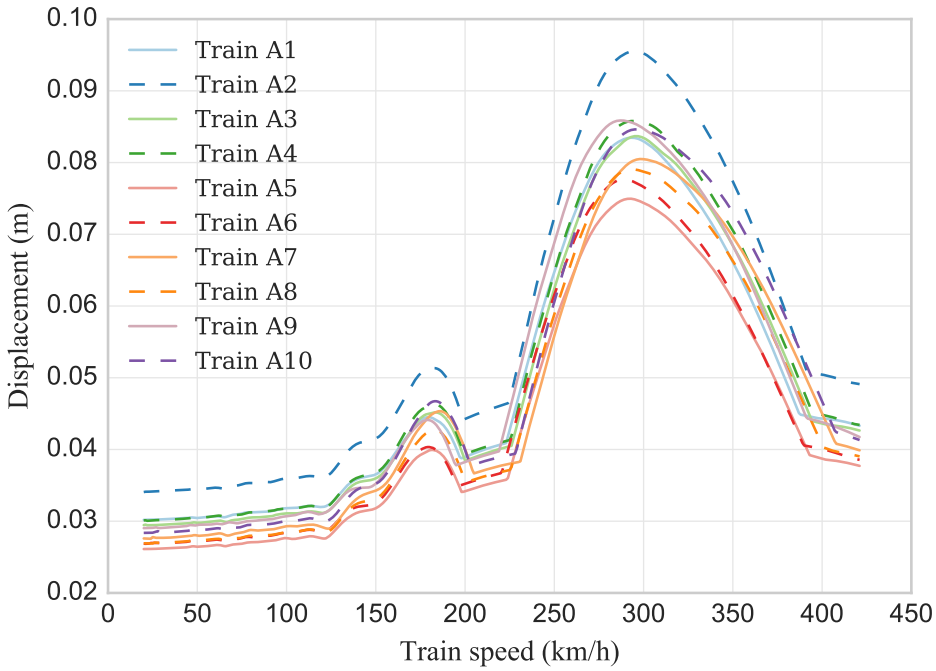

Figure 5.13: Displacement envelope curves at post-processing point on span 12 for model 4.

Finally table 5.5 shows the details of the computation. Mainly due to the difference in the number of modes, but also in the number of nodes of the line load, the performance time for the simplified model is more than five times shorter than for the complete model.

Table 5.5: Performance information.

	Model 3	Model 4
Line load nodes	87	219
Post-procesing points	108	122
Modes < 30 Hz	335	681
Performance time (CPU real time)	11h 8' 9.88"	57 h 31' 3.68"

5.5 Model with SSI Vs Model without SSI

This section also presents the temporal series obtain in the analysis of two of the five models: model 3 and model 5. In this case both models have a deck formed with 2D elements and both are simplified models. Then the difference between them lies in the foundation: model 3 is a model of the isolated arch in which the foundation is represented by an embedding and model 5 represents the soil-structure interaction. Therefore, the aim of this section is compare a model considering SSI with the same model without SSI.

There have been developed the analysis of the the passage of the train A1 at a speed of $300\,$km/h. In this case the load is applied over the right rail, in order to represent real train loads. Also it is remarkable to say that in these analysis the contribution of all vibration modes with a frequency lower than $30\,$Hz are considered.

Figure 5.14 shows the temporal solution in terms of acceleration and displacement for models 3 and 5. Actually the difference between both solutions are negligible. The temporal series of acceleration for model with soil-structure interaction is a little more dampened in the free vibration zone. In the case of the temporal series of displacement, even the curve for model 5 present moderately higher peak values.

Model 5 consider additional damping ratios because of the soil-structure interaction. This variable ratios are added to the 2% damping ratio assigned to the material. Therefore, the expected solution should be smaller in amplitude and damped earlier in time than the solution of the model without SSI. However, if the stiffness assigned to the foundation is to much restrictive and it does not moves during the passage of the load, the additional damping is minimal and it has almost no effect. Maybe this is the reason why the response of models 3 and 5 are so much similar.

To conclude, in this case more detailed characterization of the parameters that model the foundation is needed, and also a sensitivity study of these parameters.

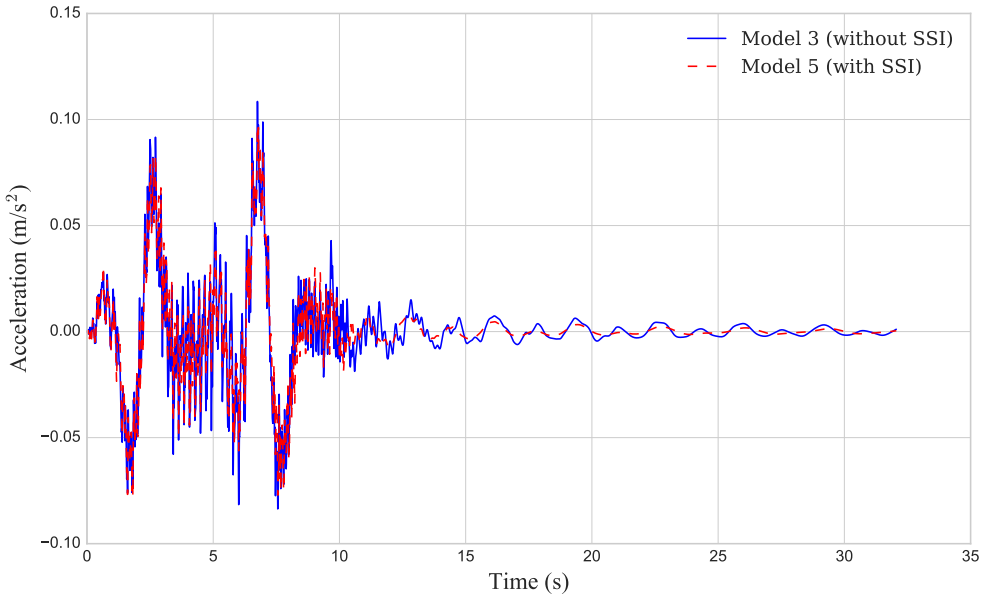

(a) Temporal series of acceleration.

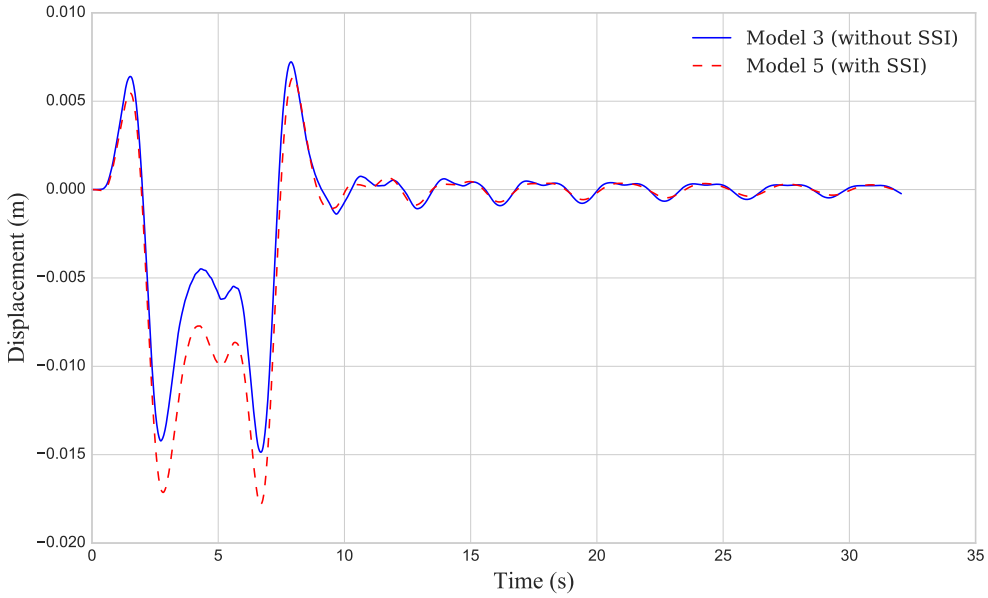

(b) Temporal series of displacement.

Figure 5.14: Results at center point of the arch due to train A1 passing at 300 km/h.

CHAPTER

6

Conclusions and future works

6.1 Concluding remarks

This document presents a detailed analysis of the dynamic problem of railway arch bridges through a case study. The semi-analytic method have been used as a tool and several FE models have been developed with the aim of get the suitable one for this kind of problems. The following points summarize the conclusions and contributions reached throughout the development of this work:

About the semi-analytic method

- The semi-analytic method has proven advantages in terms of precision and performance time compared to incremental step-by-step integration methods to solve moving load problems.
- This methodology allows to face, in a realistic way, the load steps of 1 km/h recommended by the Eurocode, which is a necessary step to determine with precision the dynamic response of HSR bridges. This method allows to perform a complete dynamic analysis of the ten trains defined in the instruction

for all speeds in a few days, for a large FE model. Time required by a step-by-step approach to solve these problems could be prohibitive.

About HSR arch bridges

- Behaviour of the viaduct is totally conditioned by the response of the arch.
- Arch modes are uncoupled from the rest of the viaduct modes. Furthermore, this arch modes appear first, so they are low frequency modes.
- High frequency modes are flapping modes of the edge flanges that are unrealistic because of the presence of the fencing at this location.

About different FE models

- Models with elements 1D are accurate and a good starting point. Although it is difficult to represent the real location of the moving load (eccentric load) in a beam deck, this kind of models are lighter and make it possible to obtain solutions quite close to those obtained with more complex models. Due to this, they are useful models in the early stages of design, to fit the main characteristics of the structure.
- Isolated arch models are a good election to represent the behaviour of viaducts such as the Almonte bridge. They are lighter than complete models and the vibration response obtain with them is quite accurate in relation to the complete model one. The relative error between both displacement solution is less than 1.5%. In addition, in this case, the performance time (CPU real time) for the complete dynamic analysis of the arch model is 5 times smaller than the time spent in the complete model analysis. For all these reasons, it can be concluded from this analysis that the isolated arch models are the most suitable ones for the study of this type of dynamic problems.
- The implementation of the soil-structure interaction in FE models is an interesting issue. In this work initial steps have been taken to address the problem. Stiffness matrix and damping ratios have been obtain, but a sensitivity analysis of its values must be carry out in order to obtain more informed conclusions of the SSI effects in HSR bridges.

6.2 Future works

The work presented in this document represents an advance on how to carry out dynamic analysis of HSR bridges. Nevertheless, much remains to be done in this area. Next, some future works are presented:

- It would be important to develop more dynamic analysis of arch bridges because there is not so many of them in the literature. This kind of bridges are a suitable solution for HSR bridges, so knowing its dynamic response is important. Perhaps a better understanding of them would help to improve their design.

- Once proven that the semi-analytic method is a very appropriated tool for the complete dynamic analysis of bridges, its use should be more widespread. That's include the analysis of other kind of bridges such as cable-stayed bridges or suspension bridges. In these examples the semi-analytic method could once again prove its advantages.

- A future work that is suggested directly from this work would be to carry out the performance of the complete dynamic analysis of the model that include soil-structure interaction. This would serve to conclude how long the effect of SSI affects on the maximum vibration experienced by the bridge over the Almonte river.

- Another line of future research could be the mathematical modeling of the soil-structure interaction itself. Although there are many scientific papers dedicated to impedances issue, maybe it would be interesting to complete the study developing a model updating of a foundation. In other words, to validate mathematical models that define the impedance values by testing a real foundation.

Bibliography

[1] A. E. Martínez Castro, P. Museros, and A. Castillo Linares. Semi-analytic solution in the time domain for non-uniform multi-span bernoulli-euler beams traversed by moving loads. *Journal of Sound and Vibration*, 294(1-2):278–297, 2006.

[2] España. Dirección General de Ferrocarriles. Instrucción de acciones a considerar en puentes de ferrocarril (iapf), 2008.

[3] J. Domínguez. *Dinámica de puentes de ferrocarril para alta velocidad: métodos de cálculo y estudio de la resonancia*. PhD thesis, 2001.

[4] British Standard. Eurocode 1: Actions on structures—, 2005.

[5] A. Kriloff. Über die erzwungenen schwingungen von gleichförmigen elastischen stäben. *Mathematische Annalen*, 61(2):211–234, 905.

[6] F. Bleich. *Theorie und Berechnung der eisernen Brücken*. Springer, 1924.

[7] J. Biggs. *Introduction to structural dynamics*. Mc Graw-Hill, 1964.

[8] Y.B. Yang, J.D. Yau, and L.C. Hsu. Vibration of simple beams due to trains moving at high speeds. *Engineering structures*, 19(11):936–944, 1997.

[9] L. Frỳba. Vibration of solids and structures under moving loads. *Telford, London*, 1999.

[10] Y.H. Chen and C.Y. Li. Dynamic response of elevated high-speed railway. *Journal of bridge engineering*, 5(2):124–130, 2000.

[11] K. Henchi, M. Fafard, G. Dhatt, and M. Talbot. Dynamic behaviour of multi-span beams under moving loads. *Journal of sound and vibration*, 199(1):33–50, 1997.

[12] R.W. Clough and J. Penzien. Dynamics of structures, 1993.

[13] N.M. Newmark. A method of computation for structural dynamics. *Journal of the engineering mechanics division*, 85(3):67–94, 1959.

[14] K. Liu, E. Reynders, G. De Roeck, and G. Lombaert. Experimental and numerical analysis of a composite bridge for high-speed trains. *Journal of Sound and Vibration*, 320(1):201–220, 2009.

[15] Y.A. Dugush and M. Eisenberger. Vibrations of non-uniform continuous beams under moving loads. *Journal of Sound and vibration*, 254(5):911–926, 2002.

[16] P. Museros, A.E. Martínez-Castro, and A. Castillo-Linares. Design goes up a gear. *Bridge. Design & Engineering*, 33:42–43, 2003.

[17] P. Museros, A.E. Martínez Castro, and A. Castillo Linares. Solución semi-analítica al problema de paso de trenes de alta velocidad sobre puentes hiperestáticos de sección variable. In *Actas del VI Congreso de Métodos Numéricos en Ingeniería, Lisboa*, 2004.

[18] P. Museros, A. Martínez Castro, and A. Castillo Linares. Semi-analytic solution for nonuniform euler-bernoulli beams under moving forces. In *Proceedings of the 7th International Conference on Computational Structures Technology, Lisboa*, volume 294, pages 278–297, 2004.

[19] A. Castillo Linares, M. Villameriel Fernández, G. Montero Poyatos, M. García Ramírez, J. de Dios Moreno Jiménez, and A. Martínez-Castro. Puente arco sobre la línea de alta velocidad córdoba-málaga. condicionantes dinámicos y constructivos para el dise-o. *Hormigón y acero*, 61(258):25–42, 2010.

[20] R.W. Clough and E.L. Wilson. Dynamic response by step-by-step matrix analysis. In *Symposium on the Use of Computers in Civil Engineering, Lisbon*, 1962.

[21] E.L. Wilson, I. Farhoomand, and K.J. Bathe. Nonlinear dynamic analysis of complex structures. *Earthquake Engineering & Structural Dynamics*, 1(3):241–252, 1972.

[22] T. Hughes. *The finite element method: linear static and dynamic finite element analysis*. Prentice-Hall, 1987.

[23] O.C. Zienkiewicz and R. L. Taylor. *The finite element method*. McGraw-hill London, 1977.

[24] K.J. Bathe and H. Saunders. Finite element procedures in engineering analysis, 1984.

[25] P. Museros, A.E. Martínez-Castro, and A. Castillo-Linares. Semi-analytic solution for kirchoff plates traversed by moving loads. In *Procedings of 6th European Conference on Structural Dynamics*, pages 1619–1624. Millpress, Rotterdam, Netherlands, 2005.

[26] J. Lysmer. Analytical procedures in soil dynamics. In *ASCE Geotechnical Engineering Division Specialty Conference on Earthquake Engineering and Soil Dynamics*, volume 3, pages 1267–1313. ASCE, 1978.

[27] J. M. Roesset. Stiffness and damping coefficients of foundations. In *Dynamic response of pile foundations: Analytical aspects*, page 30. ASCE, 1980.

[28] A. Pais and E. Kausel. Approximate formulas for dynamic stiffnesses of rigid foundations. *Soil Dynamics and Earthquake Engineering*, 7(4):213–227, 1988.

[29] G. Gazetas. Formulas and charts for impedances of surface and embedded foundations. *Journal of geotechnical engineering*, 117(9):1363–1381, 1991.

[30] B. B. Guzina, R. Y. S. Pak, and A. E. Martínez Castro. Singular boundary elements for three-dimensional elasticity problems. *Engineering Analysis with Boundary Elements*, 30(8):623–639, 2006.

[31] Instrucción del Hormigón Estructural. Ehe-08. *Madrid, Ministerio de Fomento, Secretaría General Técnica*, 2008.